Environmental Science Nano

ROYAL SOCIETY OF CHEMISTRY

PAPER

View Article Online
View Journal | View Issue

Check for updates

Cite this: *Environ. Sci.: Nano*, 2022, **9**, 375

Surface functionalisation-dependent adverse effects of metal nanoparticles and nanoplastics in zebrafish embryos†

Iris Hansjosten,‡[a] Masanari Takamiya,‡[a] Juliane Rapp,[a] Luisa Reiner,[a] Susanne Fritsch-Decker,[a] Dorit Mattern,[a] Silvia Andraschko,[a] Chantal Anders,[a] Giuseppina Pace,[a] Thomas Dickmeis,[a] Ravindra Peravali,[a] Sepand Rastegar,[a] Uwe Strähle,[a] I.-Lun Hsiao,[b] Douglas Gilliland,[c] Isaac Ojea-Jimenez,[c] Selina V. Y. Ambrose,[d] Marie-France A. Belinga-Desaunay-Nault,[e] Abdullah O. Khan,[e] Iseult Lynch,[e] Eugenia Valsami-Jones,[e] Silvia Diabaté[a] and Carsten Weiss*[a]

The growing number of manufactured nanomaterials (MNMs) used in consumer products and industrial applications is leading to increased exposures whose consequences are not yet fully understood in terms of potential impacts on human and ecosystem health. Thus, there is an urgent need to further develop high throughput testing for hazard prediction in nanotoxicology. The zebrafish (*Danio rerio*) embryo has emerged as a vertebrate model organism for nanotoxicity studies, as it provides superior characteristics for microscopy-based screening and can describe the complex interactions of MNMs with a living organism. Automated microscopy coupled with image acquisition has facilitated hazard assessment of chemicals by quantification of various endpoints (*e.g.*, mortality, malformations, hatching), an approach which we employed here to address adverse effects of a selected library of MNMs of different compositions and surface functionalities. We investigated metal and metal oxide MNMs with mean primary particle sizes of 5 to 50 nm, different chemical compositions (silica, ceria, titania, zinc oxide and silver) and various surface coatings/functionalisation, including OECD reference materials. In addition, we tested as representatives of nanoplastics polystyrene and polymethylmethacrylate nanoparticles which were surface modified by either amino- or carboxyl-groups. Our systematic analysis to establish quantitative property–activity relationships revealed a pronounced toxicity of silver and amino-modified polystyrene nanoparticles (NPs), evidenced by reduced survival and malformations. Interference with hatching, however, was the most sensitive endpoint, as zinc oxide as well as silver NPs reduced hatching already at lower concentrations (*i.e.*, 0.5 and 1 μg mL^{-1}, respectively) and early time points (3 days post fertilization, dpf). Interestingly, carboxylated polystyrene NPs and carboxylated or amino-modified polymethylmethacrylate NPs were non-toxic, highlighting both surface modification and core chemistry of nanoplastics as key determinants of biocompatibility.

Received 31st March 2021,
Accepted 10th November 2021

DOI: 10.1039/d1en00299f

rsc.li/es-nano

Environmental significance

The identification of toxic properties of manufactured nanomaterials provides the basis for the safe-by-design concept and is essential to reduce the environmental impact of chemicals, which is nowadays also referred to as green chemistry. As aquatic organisms such as fish are exposed and vulnerable to micropollutants, we screened the effects of a diverse library of nanomaterials in zebrafish embryos. Soluble metal nanoparticles and amino-functionalised polystyrene particles are identified as most hazardous. In addition to malformations and lethality, inhibition of hatching turns out to be the most sensitive endpoint. Systematic hazard profiling of nanomaterials in zebrafish embryos thus enables pinpointing of the nanomaterials' physico-chemical properties which might be also of concern to other organisms and targets for safe by design optimisation of nanomaterials properties.

[a] *Karlsruhe Institute of Technology (KIT), Institute of Biological and Chemical Systems – Biological Information Processing, Hermann-von-Helmholtz-Platz 1, 76344 Eggenstein-Leopoldshafen, Germany. E-mail: carsten.weiss@kit.edu; Tel: +49 721 60824906*
[b] *School of Food Safety, College of Nutrition, Taipei Medical University, No. 250, Wuxing St., Taipei 11031, Taiwan*
[c] *European Commission, Joint Research Centre (JRC), Via E. Fermi 2749, I-21027 Ispra, VA, Italy*
[d] *Promethean Particles Ltd., 1–3 Genesis Park, Midland Way, Nottingham, NG7 3EF, UK*
[e] *University of Birmingham (UoB), School of Geography Earth & Environmental Sciences (GEES), Edgbaston, Birmingham, B15 2TT, UK*

† Electronic supplementary information (ESI) available. See DOI: 10.1039/d1en00299f

‡ Equal contribution.

Introduction

Despite the advantages offered by cellular screening, simplistic *in vitro* systems often fail to detect more complex organ-specific toxicity. Therefore, zebrafish (*Danio rerio*) embryos may be used as an additional model that can be fine-tuned for toxicity testing and hazard ranking of chemicals including MNMs.[1] Specific advantages of this model are *ex vivo* development and transparency, short generation time, low running costs and space requirements, accessibility to genetic manipulations, and very well-studied embryo development.[2,3] The zebrafish genome has a high similarity to the human genome,[4] and the use of zebrafish embryos as an alternative model organism fully complies with the efforts to replace animal experiments as laid out in the 3R ("Replacement, Reduction and Refinement") concept.[2]

The OECD guideline No. 236 for toxicity testing of chemicals using zebrafish embryos[5] defines the testing conditions and endpoints required to generate comparable results, which can be adopted for the assessment of manufactured nanomaterials (MNMs).[6]

Metal and metal oxide MNMs are already in commerce with a high production volume and are widely applied in consumer products, leading to their inclusion in the priority list of OECD reference materials[7] for which risk assessment is urgently needed. Out of the 13 MNMs included in the list, 8 represent metal-based MNMs (silver, gold, iron, titanium dioxide, aluminium oxide, cerium oxide, zinc oxide, and silicon dioxide), whereas the remainder include carbon nanotubes, nanoclay, dendrimers, and fullerenes. Apart from the potential impact on human health, the environmental fate and safety of MNMs has been in focus since the field of nanotoxicology was established.[8,9]

Some MNMs might end up in wastewater by washing of MNMs containing clothes, for example. Due to their small size they may pass through sewage treatment plants and be released to surface waters.[10] There they are potentially hazardous to aquatic organisms like fish. For this study we selected 5 of the OECD representative materials (silicon, titanium and cerium dioxide as well as soluble silver and zinc oxide NPs[7]) which we previously tested for adverse effects in different mammalian cell lines.[11] Cationic, amine-modified polystyrene NPs were included as a representative of nanoplastics with known toxicity in most cell culture studies due to their positive surface charge.[11–13]

The zebrafish embryo is protected by the chorion, an acellular three-layered envelope with a thickness of 1.5–2.5 μm, composed of polypeptides. It has conic pores of 0.5 to 0.7 μm in diameter,[14] through which MNMs and NPs could pass because of their small size. However, there are also studies that suggest that the chorion can hinder or completely prevent the passive uptake of large molecules or particles.[15] For instance, it has been demonstrated that the chorion blocks the uptake of some larger NPs (>50 nm), *e.g.*, SiO_2 and TiO_2 NPs, but that sufficiently small and non-agglomerated Ag NPs (<50 nm) can pass through the chorion pore channels.[16–18]

In addition to size influencing bioavailability and hence potential toxicity, the chemical composition of MNMs plays an important role in determining adverse effects. Specifically, metal ions released from soluble Ag and ZnO NPs are key descriptors to explain the increased hazard of soluble *versus* insoluble metal-based MNMs.[19] At present, silver- (Ag) NPs are the best studied MNMs and are shown to be toxic to zebrafish embryos.[20–22]

Ag NPs are partly soluble in different exposure media and within target organisms.[23,24] Ag NPs (13 nm) were shown to provoke malformations and death in zebrafish embryos starting at a concentration of 15 μg mL^{-1}.[19] Citrate or polyvinylpyrrolidone-coated Ag NPs (10 nm) induced neuro-behavioural changes as assessed by the swimming behaviour in larvae after exposure to different light conditions.[25] Induced mortality, malformations, delayed hatching, and depressed heart rate seem to be linked to oxidative stress.[26,27] When compared to equimolar concentrations of soluble Ag^+ (applied as $AgNO_3$), the ion is more toxic than the NP form (8 nm Ag NPs stabilized by polyacrylate sodium).[28] Intentional coating by different chemicals or natural organic matter (NOM) also influences the colloidal stability and solubility of Ag NPs, and it can thereby modulate toxicity.[29] Also shape seems to influence the biocompatibility of Ag NPs, as Ag nanoplates were more toxic than nanospheres and nanowires in spite of their lower rates of dissolution and bioavailability. This was explained by the higher surface reactivity of the Ag nanoplates.[26]

Similar to silver MNMs, ZnO NPs are partly soluble in aqueous media and within cells.[30] Zinc is an abundant and essential transition metal in biological systems, which plays an important role in the maintenance of protein structure and enzymatic function. However, excessive free Zn^{2+} ions are toxic and are therefore bound by Zn-binding proteins, such as metalloproteins.[31] ZnO NP uptake into endosomes, with their final destination in acidifying lysosomes, accelerates their dissolution. The intracellular Zn ions induce lysosomal and mitochondrial damage as well as ROS and cytokine release.[32] In zebrafish embryos, ZnO NPs trigger adverse effects as evidenced by developmental defects and interference with hatching, most likely mediated by soluble zinc ions.[19,33,34]

Although insoluble metal-based MNMs are generally considered to be non-toxic in zebrafish, some exceptions to the rule were reported previously and are illustrated next for the MNMs used in this study. There are contradictory observations in zebrafish embryos regarding hatching, development or mortality, with silica NPs being classified either as non-toxic[17] or highly toxic.[35,36] Differences in synthesis routes and surface functionalisation of the investigated silica NPs might explain the discrepant findings, as increasing evidence links high temperature synthesis routes, leading to nearly free silanols, with increased toxicity.[37,38]

Bar-Ilan *et al.* observed embryo malformation and mortality when zebrafish embryos were exposed simultaneously to different TiO_2 NPs and UV light, while exposure to TiO_2 NPs in the dark was non-toxic.[16,39,40] In the presence of UV light, the TiO_2 NPs were phototoxic due to generation of ROS which induced adverse effects.

CeO_2 NPs were found to be non-toxic to zebrafish embryos in several studies.[41–43] However, rod shaped CeO_2 NPs damaged the epithelial lining of the gastro-intestinal tract in zebrafish larvae at 14 dpf, interfering with growth and development, while spherical particles had no effect.[44]

Plastic pollution of the environment is an emerging threat to ecosystems, and in recent years the deleterious impact of microplastics (*i.e.* particles smaller than 5 mm) on several aquatic organisms has been documented.[45–47] Less is known for nanoscale plastics (*i.e.* particles smaller than 1 μm or 100 nm depending on the definition utilised) with respect to environmental fate and safety.[48–50]

Some studies have investigated the toxicity of polystyrene (PS) NPs, one of the most abundant plastics, in different aquatic organisms.[51–53] In zebrafish embryos, non-functionalised, fluorescent PS NPs (51 nm) accumulated in the yolk sac and were distributed to various organs (intestine, gallbladder, liver, heart, brain, pancreas) without triggering lethality or malformations but provoking bradycardia and hypoactivity.[54,55] Although non-functionalised PS NPs (20 and 50 nm) were found not to be acutely toxic to zebrafish, they serve as a carrier for persistent organic pollutants and increase their uptake and toxicity.[56,57] Interestingly, immunocompromised and infected larvae are hypersensitive to PS NPs, evidenced by reduced survival.[58] As no reference has been found reporting on the toxic action of surface-modified polystyrene NPs in zebrafish embryos and larvae, we included amine- and carboxyl-modified polystyrene (PS-NH_2 and PS-COOH) NPs in our analysis. Both have been used extensively to study the toxic mechanism of action in cell lines and its dependence on surface functionalisation.[11–13,59,60] Whereas PS-NH_2 NPs are highly cytotoxic, PS-COOH appear biocompatible in cells. The positive surface charge of PS-NH_2 NPs leads to lysosomal acidification and damage, which eventually culminates in cell death.

In this study, automated microscopy combined with automated image acquisition was employed to quantitatively assess different phenotypes upon MNM exposure (*i.e.* lethality, hatching). To this end, one embryo per well was exposed to a defined concentration of MNMs and individually imaged for up to 5 dpf. Such high throughput plate-based assays are routinely used to screen effects of MNM libraries in cell culture,[11,12] but are rarely applied to study toxicity in zebrafish embryos. Usually, a batch of embryos (*e.g.*, 10–20) is exposed and individual responses are not recorded. Also, during exposure dead embryos need to be removed, which would otherwise have an impact on the remaining fraction. In previous studies we were able to monitor the detrimental effects in embryos exposed to toxic chemicals up to 48 hpf (hours post fertilization) by automated image analysis.[61] Here, we decided to test the utility of this approach for hazard assessment of MNMs in embryos but also larvae. The aim was to correlate the physico-chemical properties of the MNMs with their adverse effects on zebrafish embryos. For those MNMs which provoked adverse effects in the initial screening, a detailed dose–response and temporal analysis was conducted. Finally, hazard profiling in zebrafish embryos was compared to *in vitro* studies with cell lines where the same set of MNMs has been recently investigated.[11]

Materials and methods

Nanomaterials

The MNMs used in this study are all from the NanoMILE project MNM library. More specifically, the OECD reference materials TiO_2 NM-103, TiO_2 NM-104, CeO_2 NM-212, ZnO NM-110, ZnO NM-111, and Ag NM-300 K NPs, as well as the corresponding dispersant and capping agent containing 4% each of polyoxyethylene glycerol trioleate and polyoxyethylene (20) sorbitan mono-laurat (Tween 20) were provided by the JRC (Joint Research Centre, Ispra, Italy) repository and were described previously.[62–65] TiO_2-Plain, TiO_2-PVP, TiO_2-F127, TiO_2-AA4040, and CeO_2-plain NPs were produced by Promethean Particles Ltd. (Nottingham, UK) using a continuous-flow hydrothermal method which has been previously described in the literature,[66,67] and their characterisation has been described in Joossens, *et al.*[68] and Khan *et al.*[69] SiO_2-un, SiO_2–NH_2, and SiO_2–COOH NPs were synthesised and characterised at the JRC.[70] Various nanoplastics were investigated: PS-NH_2 NPs (Bangs Laboratory, Fishers, IN, USA), PS-COOH NPs (Polysciences Europe, Hirschberg an der Bergstraße, Germany) and polymethylmethacrylate (PMMA) NPs (Micromod Partikeltechnologie GmbH, Rostock, Germany), either amino-modified (PMMA-NH_2 NPs) or carboxylated (PMMA-COOH NPs). PS-NH_2 NPs were additionally purchased from another vendor (Sigma-Aldrich, Taufkirchen, Germany) to verify results obtained with those ordered from Bangs laboratory and were only used for the experiments depicted in Fig. S12.†

MNMs were received as aqueous suspension or as dry powder and were used as provided. For dispersion in Holtfreter's medium (60 mM NaCl, 0.67 mM KCl, 0.82 mM $CaCl_2 \cdot 2\ H_2O$, and 2.38 mM $NaHCO_3$, pH 7.0) MNMs were dispersed at 5 mg mL^{-1} in sterile filtered MilliQ water, and then diluted to the dosing concentrations shortly before exposure. Aqueous suspensions which were prepared from MNM powder were ultrasonicated for 15 min in the ultrasonic water bath Bandelin Sonorex (Bandelin, Berlin, Germany) at 250 W, while those prepared from MNM suspensions were ultrasonicated for 5 min. The stock suspensions were further diluted in Holtfreter's medium (see below). Due to the hydrophobicity of ZnO NM-111, both ZnO particles were dispersed according to the NanoGenoTox dispersion protocol:[71] Briefly, to prepare a 2.56 mg mL^{-1}

stock solution 15.6 mg MNMs were weighed and then pre-wetted with 30 μL ethanol (>96%). After gentle mixing, 970 μL of 0.05% sterile filtered bovine serum albumin (BSA, PAA, Cölbe, Germany) solution in MilliQ water was added and the suspension was carefully mixed. Then another 5 mL of 0.05% BSA solution was added (total volume 6 mL) and sonication with a tip sonifier (Branson Sonifier 250, Schwäbisch Gmünd, Germany) for 2 × 1 min (50 duty cycles, output 5) was performed. From here all dispersions were diluted in Holtfreter's medium to 2× the required exposure concentration. Before each dilution step the dispersions were mixed by pipetting or vortexing. All particles were tested at least twice for toxicity by screening experiments at 1 and 125 μg mL^{-1} in Holtfreter's medium (5 days of exposure). The dispersant for the Ag NM-300 K NPs was tested as a further control at an equivalent concentration (1 mg mL^{-1}) to match the maximal exposure concentration of Ag NM-300 K NPs (125 μg mL^{-1}). The selected concentrations were chosen based on our previous studies assessing toxicity in cell culture experiments[11] to directly compare the effects at a similar dose in zebrafish embryos. For those materials (ZnO, Ag, PS-NH_2) showing adverse effects, *i.e.*, interference with hatching and increased mortality, additional concentrations (ZnO, Ag: 2, 3.9, 7.8, 15.6, 31.3, 62.5 μg mL^{-1}; PS-NH_2: 3.9, 7.8, 15.6, 31.3, 62.5 μg mL^{-1}) were tested to obtain dose response curves.

All MNMs at the highest exposure concentration (125 μg mL^{-1} in Holtfreter's medium) have been characterised immediately following dispersion (time 0) and after 24 hours (time 24) (Table S1†). Dynamic light scattering (DLS) measurements were performed on a Malvern Zetasizer 5000 (Malvern, UK). Ten consecutive measurements were carried out and averaged to calculate the mean size. The results were obtained with samples equilibrated for 2 minutes before the measurements were started. Transmission electron microscopy (TEM) samples were prepared on copper grids by means of the drop method.[72] MNM imaging was carried out using a Zeiss TEM (EM 910, Oberkochen, Germany) and a JEOL 1200 TEM (Peabody, MA, USA).

Zebrafish husbandry and high throughput imaging

Zebrafish husbandry and crossing was performed as described previously.[73–75] Adult wild-type zebrafish (*Danio rerio*, strain: AB ZIRC KA; 1 female, 2 males per breeding cage) were allowed to spawn in facility water. Clutches were collected 1 hour after spawning and kept separately in petri dishes in facility water. Only clutches with a fertilization rate of >80% were further processed. Embryos with normal characteristics of development[73] were washed 2× with clean facility water and 1× with Holtfreter's medium, thereby removing any debris. From this point embryos were kept in Holtfreter's medium (also referred to herein as embryo medium). At sphere stage, 2–3 clutches were selected, and a sufficient number of healthy embryos were pooled into a single Petri dish using a stereomicroscope (Nikon SMZ 645). At 30% epiboly (at about 5 hpf), embryos were sorted into round bottom 96 well plates, one embryo per well in a volume of 100 μL medium. Accuracy of sorting and embryo quality were checked by visual inspection, and missing or damaged embryos were added or replaced, respectively. At 50% epiboly (at about 6 hpf), 100 μL of the 2× concentrated freshly prepared particle dispersions were added, resulting in a total exposure volume of 200 μL. As stipulated in the OECD guideline 236, we performed static exposure to minimise any additional stress to the embryos in contrast to semi-static renewal in case of unstable compounds, where the exposure concentration of ±20% of the nominal concentration cannot be maintained. The plates were kept in a moist chamber in an incubator at 28 °C, and brightfield images were acquired by the automated microscope Olympus IX81 (Olympus Lifescience, Germany) as described previously for embryos exposed to chemicals up to 48 hpf, with some modifications.[61] At 24, 48, 72, 96, and 120 hpf, brightfield images were analysed for survival and hatching (Fig. S1†). Six pictures of each well and time point were taken in *z*-planes with a distance of 100 μm. Different magnifications were used depending on the age and size of the embryos. Up to 48 hpf a 2.5× objective was used, thereafter a 1.25× objective. Every plate was imaged twice at each time point to minimize evaluation mistakes. After the final acquisition at 120 hpf the larvae were euthanised and discarded. An overview summarizing the main steps of the screening procedure is depicted in Fig. S1.†

For this study, 15 MNMs were screened at two concentrations in 12 embryos each, and two to three independent experiments were performed. With 12 images per embryo acquired every 24 h over 5 days, approximately 60 000 images were generated. For the follow-up experiments, testing of more refined dosages (up to 6) to establish dose–response curves for the ZnO-plain and ZnO-TECS (including $ZnCl_2$ as a control), Ag, PS-NH_2, and PS-COOH MNMs resulted in acquisition of an additional 120 000 images. These roughly 180 000 images (equivalent to *ca.* 600 GB of data) were processed manually and analysed by the naked eye. Per embryo, we selected usually one image out of 2 *z*-stacks of 12 images with different focal planes to obtain an optimal imaging condition for analysis, thereby reducing the data to 15 000 images. Assuming that 0.5–1 min is needed for the pre-selection of the optimal image (one out of twelve) and the manual image analysis to make a binary decision (yes/no) concerning the two read-outs, even trained experts need theoretically 125–250 hours of constant analysis, which in practice translates to several months for data processing and analysis. Automated image acquisition by the microscope demands roughly 30 min per plate, which in this screen equates to about 80 hours. In reality, this amounts again to several months of screening, as plates were imaged over 5 days each.

Histology and transmission electron microscopy

Embryos (*Danio rerio*, Tübingen AB wildtype strain) were processed as described previously.[76] Samples were fixed with

Karnovsky fixative (2.5% (w/v) glutaraldehyde, 2% (w/v) paraformaldehyde, 0.1 M PIPES pH 7.0) overnight at 4 °C. Embryos were briefly washed with 0.1 M PIPES pH 7.0 and treated with secondary fixative for 1 hour at 4 °C in 0.8% (w/v) $K_3[Fe(CN)_6]$, 0.5% (w/v) OsO_4, 0.1 M PIPES pH 7.0. The samples were contrasted with 2% (w/v) uranylacetate in 25% (v/v) ethanol at 4 °C for several days. After gradual dehydration through an ethanol series (25%, 50%, 70%, 90%, 95%, and 100%) and 1,2-propylene oxide, the samples were embedded into EPON 812 resin. Semi-thin sections (350 nm) and ultra-thin sections (70 nm) were prepared with a Leica EM UC6 ultramicrotome. For light microscopy, semi-thin sections were recovered onto a glass slide by a perfect loop (Electron Microscopy Sciences, PA) for staining with toluidine blue O (T3260, Sigma-Aldrich), followed by mounting in EPON. Images were acquired in tile scan by 63×/1.40 HCX PL APO objective with oil as immersion medium, using DM6 B upright microscope (Leica Microsystems, Wetzlar, Germany). Individual tile scan images were merged by LAS X software (Leica Microsystems). For electron microscopy, ultra-thin sections were directly recovered onto EM-slot grids (2 × 1 mm slot formvar-coated EM grids; Agar Scientific, G2500PD). Images were acquired by a transmission electron microscope (Zeiss EM910) operated at 80 kV with magnification of 25 000.

Statistics

The embryos/larvae were classified for the endpoints hatching and mortality, based on the images taken at each time point. 12 embryos were treated per condition in each experiment. A negative control (embryo medium only) was included on each plate. The percentage of hatched and dead embryos was calculated as the number of affected embryos in each treatment group, which was normalised by the total number of analysed embryos (*i.e.*, the starting number at 6 hpf) and depicted as hatching (%) and mortality (%). The normalised values were averaged for each condition, and results are reported as mean (in the case of two independent experiments) or mean ± standard error of the mean (s.e.m.) in the case of 3–5 independent experiments. Statistical significance was tested using the Student's *t*-test.

Results

Physico-chemical characterisation of MNMs

The MNMs were selected from a library of different MNMs with a size range of 5 to 50 nm, to study the impact of primary particle size on toxicity, as well as the impact of different core chemistries, coatings, and surface functionalisation (Table S1†). As metal and metal oxide MNMs have been studied previously in zebrafish as introduced above, we focussed particularly on the effects of surface coating and modifications affecting surface charge, to evaluate their impact on biocompatibility. The selected particles include SiO_2 (similar size, different surface modifications), TiO_2 (similar size, different crystal structure and surface coatings), CeO_2 (different synthesis routes and thus different characteristics), Ag (surface coated), and ZnO (similar size, hydrophobic or hydrophilic coating). PS-NH_2 NPs were included as positive control, as they are highly toxic to mammalian cells;[11,12] however, they have not been assessed so far in zebrafish embryos.

Additional representatives of nanoplastics, which were previously not tested in cell culture experiments,[11] were used to address the importance of plastic surface charge/functionalisation and core chemistry. To this end, PS-COOH and PMMA-NH_2 as well as PMMA-COOH were investigated. The COOH and NH_2 groups provide a negative or positive surface charge, respectively, whereas the core chemistry is defined by the two different synthetic polymers, *i.e.* polystyrene and polymethylmethacrylate. Whereas it is already known that cationic, amine-modified but not anionic, carboxylated PS NPs are toxic, it is not clear whether other nanoplastics composed of different polymers (*e.g.* PMMA) and these type of surface modifications would behave similarly. TEM-derived diameters confirm that all particles are in the nanometer range. *Z*-Average and polydispersity index (PDI) were determined in Holtfreter's medium (Table S1†) directly after preparing the suspension and after 24 h. The agglomeration of the MNMs differs depending on the material chemistry and surface functionalisation. With the exception of all nanoplastics, SiO_2-plain, SiO_2–COOH, and silver NPs, all other particles agglomerated in Holtfreter's medium. Of note, surface functionalisation by amine modification rendered negatively charged silica NPs colloidally unstable as documented previously.[77] Increasing numbers of amine groups might contribute to amine-silanol hydrogen bonding, thereby enhancing inter-particle attractive forces and agglomeration.[78] Further physico-chemical characterisation data of the MNMs under study can be found in Joossens *et al.*[68] Detailed reports are also available for the representative test MNMs TiO_2 (NM-103, NM-104),[62] CeO_2 NM-212,[63] ZnO (NM-110, NM-111),[64] and Ag NM-300 K (ref. 65) from the JRC repository.

LOAELs in zebrafish embryos reveal selective toxicity of amine-modified polystyrene-, zinc-, and silver-NPs

Effects on zebrafish embryos upon exposure to the selected MNMs were studied by either quantitative analysis of the hatching rate and mortality or qualitative assessment of malformations by automated microscopy. As shown in Fig. 1, SiO_2, TiO_2, and CeO_2 MNMs as well as their modifications had no effects after incubation at concentrations up to 125 μg mL^{-1} for 5 days (120 hpf). Representative images of zebrafish larvae exposed to non-toxic MNMs are shown in Fig. S2.† The lowest observed adverse effect levels (LOAELs) for reduction of hatching rate were 1 μg mL^{-1} for ZnO-plain and ZnO-TECS NPs and 3.9 μg mL^{-1} for Ag NPs, respectively. Although the Ag NPs inhibited hatching at similar concentrations as the ZnO NPs, they were much more toxic considering the mortality endpoint, for which Ag NPs showed a LOAEL of 7.8 μg mL^{-1}, while for the

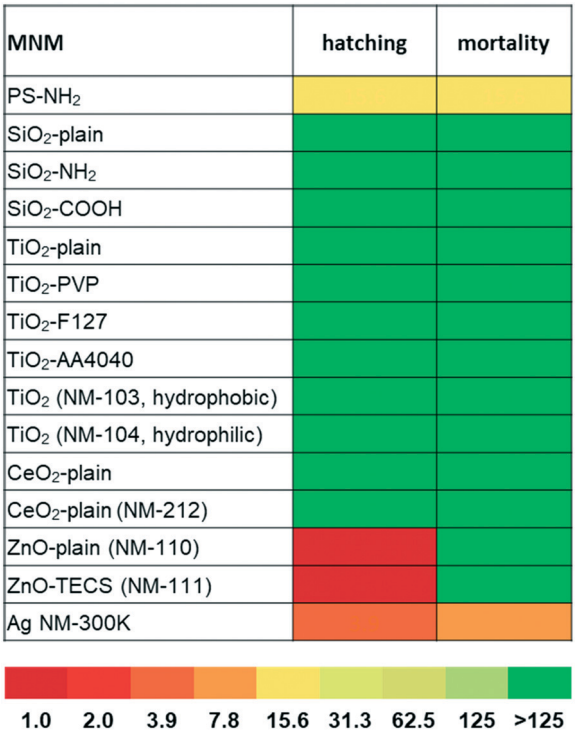

Fig. 1 Toxicity of PS-NH_2-, ZnO-, and Ag-NPs in zebrafish embryos. The heatmap depicts the lowest observed adverse effect levels (LOAELs, mean value) of MNMs for interference with hatching and mortality assessed at 120 hpf. The colour code corresponds to the LOAEL concentrations in μg mL^{-1}. All MNMs were screened twice at 1 and 125 μg mL^{-1}, and effects on 12 embryos per treatment in each experiment were analysed. Toxic MNMs were re-tested at multiple concentrations (1, 2, 3.9, 7.8, 15.6, 31.3, 62.5, and 125 μg mL^{-1}) in 2 to 5 independent experiments.

ZnO NPs no LOAELs could be defined (>125 μg mL^{-1}) (Fig. 1 and Table S2†). Thus, the Ag NPs not only prevented hatching but also killed the embryos. No adverse effects were observed for the dispersant of the Ag NPs when used at the same concentration as in the particle preparation (data not shown), which is in line with a previous publication.[6] Interestingly, amino-modified PS NPs (PS-NH_2 NPs) were also highly toxic to zebrafish embryos, with hatching inhibited and mortality induced at 15.6 μg mL^{-1} (Fig. 1).

Previously, a concordant ranking of NP toxicity could be observed when zebrafish embryo data were compared to cell culture data using the same set of MNMs.[19] In a similar attempt the cytotoxic response in two different commonly used cell lines, human HCT116 colon epithelial cells and adenocarcinomic human alveolar basal epithelial cells,[11] was correlated with embryo lethality (Fig. S3†) upon exposure to the different MNMs. Whereas the MNMs (*i.e.*, silica-, titania-, and ceria-NPs) found to be non-toxic in zebrafish neither were cytotoxic in human cells, PS-NH_2 and Ag NPs provoked toxicity in both models. Therefore, malformations and lethality provoked by PS-NH_2 and Ag NPs in zebrafish embryos could be correlated with cytotoxic effects detected in cell culture.

Time-resolved dose response analysis of embryo toxicity upon Ag NP exposure

The Ag NPs interfered with hatching, morphogenesis, and survival of the zebrafish embryos in a concentration dependent manner at 120 hpf (Fig. 2A and B, Table S2†). Inhibition of hatching depends not only on dosage but also on the exposure duration (Fig. S4†). For instance, a delay in hatching is already observed at the lowest concentration of 1 μg mL^{-1} of silver NPs at 72 hpf (Fig. 2A). Higher concentrations further delay the time of hatching, with a complete block of hatching at 125 μg mL^{-1}. Increasing Ag NP concentrations progressively disturbed morphological development, causing lethality already after 24 hpf and affecting almost all embryos at higher doses (>62.5 μg mL^{-1}) (Fig. S4 and S5†). Different types of malformations were observed but not quantified, such as pericardial oedema, bent caudal fin, and altered head morphology (Fig. S1B†).

The chorion was stained brownish on the outside whereas no staining was seen inside. The discolouring of the chorion outer surface at high concentrations of Ag NPs even obscured the view of the embryos inside (Fig. S5†).

Time-resolved dose response analysis of interference of ZnO NP exposure on hatching

Embryos were treated with ZnO-plain and ZnO-TECS particles at a lower concentration range compared to the other MNMs because interference with hatching started already at a very low concentration of 2.5 μg mL^{-1} (Fig. 3A) and high particle concentrations obscured the view onto the embryos, as already observed for Ag NPs above (Fig. S6†). Since it is known that ZnO NPs dissolve in zebrafish medium,[79] we compared the effects to those induced by soluble $ZnCl_2$ at equimolar concentrations of Zn. The analyses were done at 120 hpf. Table S3† shows the values for the LOAELs (lowest observed adverse effect levels), the NOAELs (no observed adverse effect levels), and the EC_{50} (effective concentration which induces a half maximal response). ZnO-Plain and ZnO-TECS particles prevented hatching of zebrafish embryos already at 1 μg mL^{-1}. The soluble $ZnCl_2$ also prevented hatching at 0.82 μg mL^{-1}, while morphology and survival appeared normal. When considering the equivalent Zn concentration (Fig. 3B), $ZnCl_2$ provoked a similar response as ZnO NPs already at half the dose (*i.e.* 0.4 *versus* 0.8 μg mL^{-1} Zn^{2+}). Assuming that zinc ions are responsible for the interference with hatching by directly binding to the zebrafish hatching enzyme (ZHE) as reported previously[33] the reduced efficiency of ZnO NPs might be explained by incomplete dissolution of the particles. While lower concentrations of NPs delayed hatching, at higher concentrations a gradual increase in interference up to a complete block of hatching at 125 μg mL^{-1} was noted (Fig. S8†). Hatching interference from exposure to ZnO-plain NPs was observed at earlier time points compared to ZnO-TECS NPs, indicating a lower potency of the latter which might be related to a slower dissolution of ZnO-TECS NPs due to the

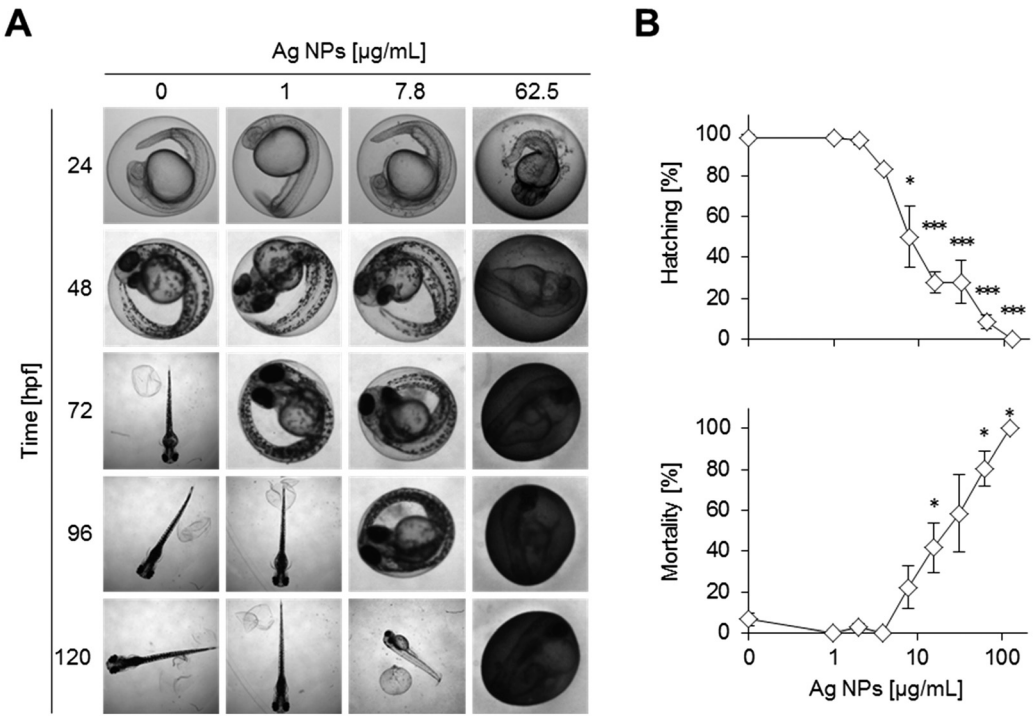

Fig. 2 Ag NPs interfere with hatching and induce mortality at low and high concentrations, respectively. Zebrafish embryos were treated with increasing concentrations of Ag NPs at 6 hpf and analysed at the indicated time points. Controls were exposed to Holtfreter's medium only (0 µg mL^{-1}). (A) Representative images to illustrate inhibition of hatching, mortality, and malformations (and discolouration of the chorion due to particle attachment). (B) Hatching and mortality, normalised to the total number of analysed embryos, are shown as a function of MNM exposure concentration after 120 hpf, shown as the means of 3 to 5 experiments ± s.e.m. Note that for the concentration 3.9 µg mL^{-1} only one experiment was available (*$p < 0.05$, ***$p < 0.001$).

coating (Fig. S7 and S8†). In addition, we analysed the body length of larvae at 5 dpf which were either untreated (control) or exposed to ZnO NPs. As the latter did not hatch, the chorion was removed to properly image the larvae. Indeed, the body length of unhatched embryos was reduced compared to controls to about 8–10% (Fig. S9†).

PS-NH_2 NPs but not PS-COOH NPs are acutely toxic to zebrafish embryos

PS-NH_2 NPs were highly toxic in zebrafish embryos (Fig. S10A and C and S11A†). After 24 hpf, exposure to 31.2 or 62.5 µg mL^{-1} PS-NH_2 NPs resulted in more than 80% mortality (Fig. S10C†). At 48 hpf, lower concentrations of PS-NH_2 NPs, *i.e.*, 3.9 and 7.8 µg mL^{-1}, were non-toxic whereas at the higher concentrations (31.2 and 62.5 µg mL^{-1}) hatching was inhibited (Fig. S10A and S11A†) and none of the embryos survived (Fig. S10C and S11A†). Interestingly, a strong impact on the survival of larvae could also be seen upon exposure to 15.6 µg mL^{-1} PS-NH_2 NPs, which provoked 70% lethality at 120 hpf (Fig. S10C and S11A†). As surface modification of PS NPs by carboxylation suppresses adverse effects in cell culture experiments,[59,60] we tested PS-COOH NPs at the highest concentrations of 31.2 and 62.5 µg mL^{-1} for toxicity in zebrafish embryos/larvae. Interestingly, no toxicity could be observed up to 120 hpf (Fig. S10B and C and S11B†). As revealed in histological sections, PS-NH_2 NPs but not PS-COOH NPs induced cell death in zebrafish embryos (Fig. 4). To further corroborate the pronounced toxicity of amino-modified polystyrene, PS-NH_2 NPs with a similar size purchased from another supplier were studied (Fig. S12†). Again, a dose dependent impact on mortality upon exposure to PS-NH_2 NPs became evident. In order to address the importance of core chemistry on nanoplastic toxicity, amino- or carboxy-modified polymethylmethacrylate (PMMA) NPs of comparable size to the PS NPs were also used. Surprisingly, PMMA-NH_2 NPs were non-toxic and no difference in comparison to the PMMA-COOH NPs could be seen (Fig. 5A–C). The level of surface coverage by amino-groups has recently been identified as a key parameter driving adverse effects of silica NPs in mammalian cells.[77] The relative amounts of amino-groups on the surface of PS-NH_2 and PMMA-NH_2 NPs were quantified and found to be in a similar range (Table S4†). Hence, the striking difference in the toxicity between PS-NH_2 and PMMA-NH_2 NPs illustrates that not only the surface modification but also the core chemistry of nanoplastics needs to be considered for hazard assessment.

Discussion

Automated microscopy combined with automated image acquisition was employed for quantification of adverse phenotypes in zebrafish embryos (*i.e.*, lethality and inhibition of hatching) upon MNM exposure. A variety of MNMs with

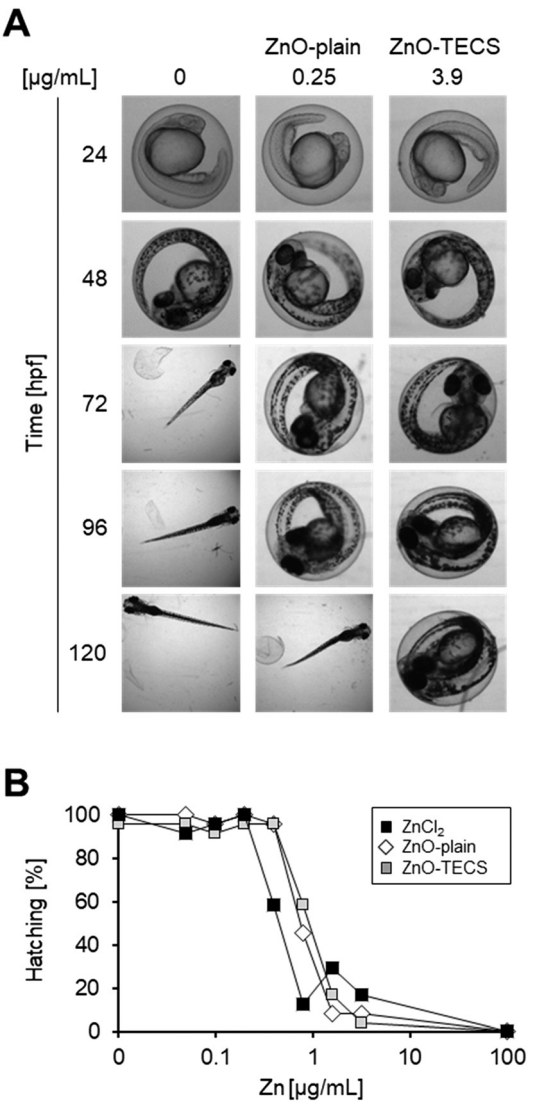

Fig. 3 ZnO NPs and zinc chloride interfere with hatching of zebrafish embryos. Zebrafish embryos were treated with ZnO-plain, ZnO-TECS, and $ZnCl_2$ at equimolar Zn concentrations at 6 hpf and the percentage of hatched embryos was analysed at the indicated time points. Controls were exposed to Holtfreter's medium only (0 µg mL^{-1}). (A) Representative images to illustrate inhibition of hatching by ZnO NPs. (B) Dose-dependent decrease of hatching after exposure to ZnO NPs and $ZnCl_2$ at equivalent concentrations of Zn, depicted as the mean values of two independent experiments.

different core chemistry, surface functionalisation, and coatings was investigated to identify critical physico-chemical properties which are essential to enable a safe-by design approach in the future. In the following we first consider the advantages and limitations of microscopy-based high throughput screening (HTS) for hazard assessment in zebrafish embryos, and its future perspectives. Secondly, we discuss the literature on those MNMs found to be non-toxic in our studies, before turning to the MNMs with potent toxicity *i.e.*, ZnO and Ag NPs. Finally, we also focus our attention on nanoplastics as emerging environmental pollutants.

Potential, limitations, and perspectives of hazard profiling of MNMs by high throughput imaging in zebrafish embryos

Whereas the speed of automated microscopy seems to be fairly optimised and reaching its limits, requiring the parallel use of multiple quite expensive screening microscopes for even faster throughput, there seems to be a clear need for improved automated image analysis. In our studies, the acquisition and analysis of thousands of images was much more time consuming than simply looking at the plates and scoring the two phenotypes. However, with the recent drive to optimally use data according to the FAIR (findable, accessible, interoperable and reusable) principle,[80] it is a prerequisite to establish procedures that provide raw images which enable an unbiased image analysis also of more complex morphological read-outs, *e.g.*, by machine learning.[81] Software has been developed to monitor toxicity by many optical read-outs and morphological phenotypes, *e.g.*, coagulation (death) or changes in the heart rate of embryos.[61,82] Analysis of standard bright-field images relies on grey scale pixel intensities for feature extraction and object detection. However, in the case of agglomerated and precipitated MNMs, images are often blurred, and objects (*e.g.*, embryo or chorion) are not easily correctly assigned. Nevertheless, hatching rate (in the absence of MNM agglomerates) can be determined with an accuracy of more than 94%.[83] For the automated assessment of coagulation,[61] gentle washing and exchange of MNM containing medium at a given time or pulse-chase experiments (*i.e.*, transient application of MNM for a defined time interval) would presumably solve the problem. In our studies, the impact of ZnO, Ag and PS-NH_2 NPs on malformations could not be quantified as the interaction of the particles with the chorion impedes acquistion of images depicting the entire bodyshape. Furthermore, these MNMs interfered with hatching. Unhatched embryos and larvae are curled and twisted inside the chorion due to space constraints and therefore complete assessment of malformations is challenging. For more detailed investigations on morphological malformations embryos need to be dechorionated and correctly positioned in order to properly image the region of interest. Apart from bright-field images, fluorescence can be monitored in transgenic lines with labelling of specific cells in specific organs, for example. Additionally, many reporter lines employing fluorescent protein markers linked to specific signalling pathways are available to measure the effect of chemicals or MNMs on certain genes relevant for mechanistic investigations into toxicity pathways. Such approaches have been used previously to successfully monitor the expression of various promoter-enhancer combinations in different tissues in high-throughput.[84] In this way, agglomerated non-fluorescent MNMs should interfere less with fluorescent read-outs and could be screened for more sophisticated effects and modes of action in living zebrafish.

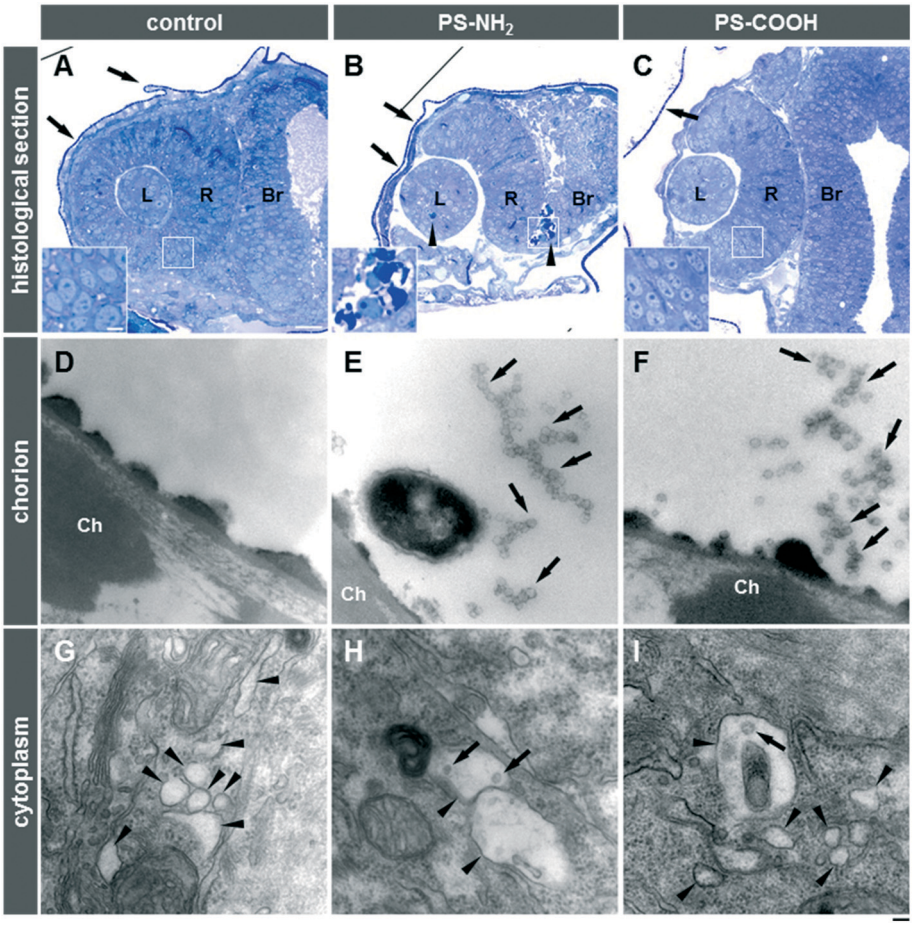

Fig. 4 Histological and ultrastructural analysis to assess adverse effects and localization of nanoplastics in zebrafish embryos. Zebrafish embryos were exposed to 31.3 μg mL^{-1} PS-NH_2 or 62.5 μg mL^{-1} PS-COOH. Controls were exposed to Holtfreter's medium alone. (A–C) Toluidine blue-stained histological sections (transverse [A and B]; horizontal [C]) at the level of the eye from untreated (A), PS-NH_2 (B), or PS-COOH (C) treated embryos (6–24 hpf; n = 3 embryos for each treatment) are shown. Note the presence of dark-stained nuclei (arrowheads) indicative of cell death after the PS-NH_2 treatment. The lens (L), retina (R), brain (Br), and chorion (arrows) are indicated. (Insets) Magnified views from white squared regions to show cell nucleus morphology. Scale bars: 25 μm (A–C) and 5 μm for insets. (D–I) Ultrastructure analysis of the chorion (Ch; D–F) and the skin epithelium (G–I) from untreated embryos (D and G), PS-NH_2-treated (E and H), and PS-COOH-treated zebrafish embryos (F–I). (D–F) NPs of about 50 nm diameter (arrows) were spotted in PS-NH_2 (E) or PS-COOH (F)-treated embryos on the outer surface of the chorion, while none could be observed in untreated embryos (D). (G–I) Intracellular vesicles (arrowheads) and NPs (arrows) were observed in the skin epithelium of NP-treated embryos (H–I). (D–I) Scale bar: 100 nm.

A robotics approach which allows automatic loading of zebrafish larvae from multi-well plates, and positions and orients them for high-speed confocal imaging with cellular resolution[85] would potentially be very useful to assess the effects (*e.g.* malformations) of MNMs by high-throughput imaging, yet this is technically much more demanding and requires removal of the chorion prior to imaging. Such a system for automated positioning of zebrafish embryos/larvae could also be combined with bright-field imaging to allow automated, image-based feature assessment.[86] A newly developed software (FishInspector) enables quantification of several morphological parameters (*e.g.*, eye size, body length, yolk sac size, otolith-eye distance, pericardial size, tail malformations, swim bladder inflation, head size). Alternatively, luminescence is used to quantify differences in gene expression[87] or signaling pathway activity in high-throughput, where detection does not require spatial optical resolution as obtained by a microscope,[88] and such assays could be adapted for more refined studies on the molecular action of MNMs.

From the above discussion it is also clear that the screening of only 15 MNMs by HT imaging already generates so much data that assessment of large MNM libraries of up to a few thousand MNMs combined with different exposure conditions (*e.g.*, presence of natural organic matter, UV radiation, salinity, mixture of pollutants, *etc.*) is not feasible at present. Therefore, a tiered approach is needed, whereby pre-screening of MNMs using simple targeted read-outs at defined developmental stages is performed (*e.g.*, coagulation at 48 hpf). MNMs which scored positively in such assays can then be more rigorously tested, *e.g.*, at higher spatiotemporal resolution down to the cellular level[60,89,90] and with multiple dosages, albeit at lower throughput.

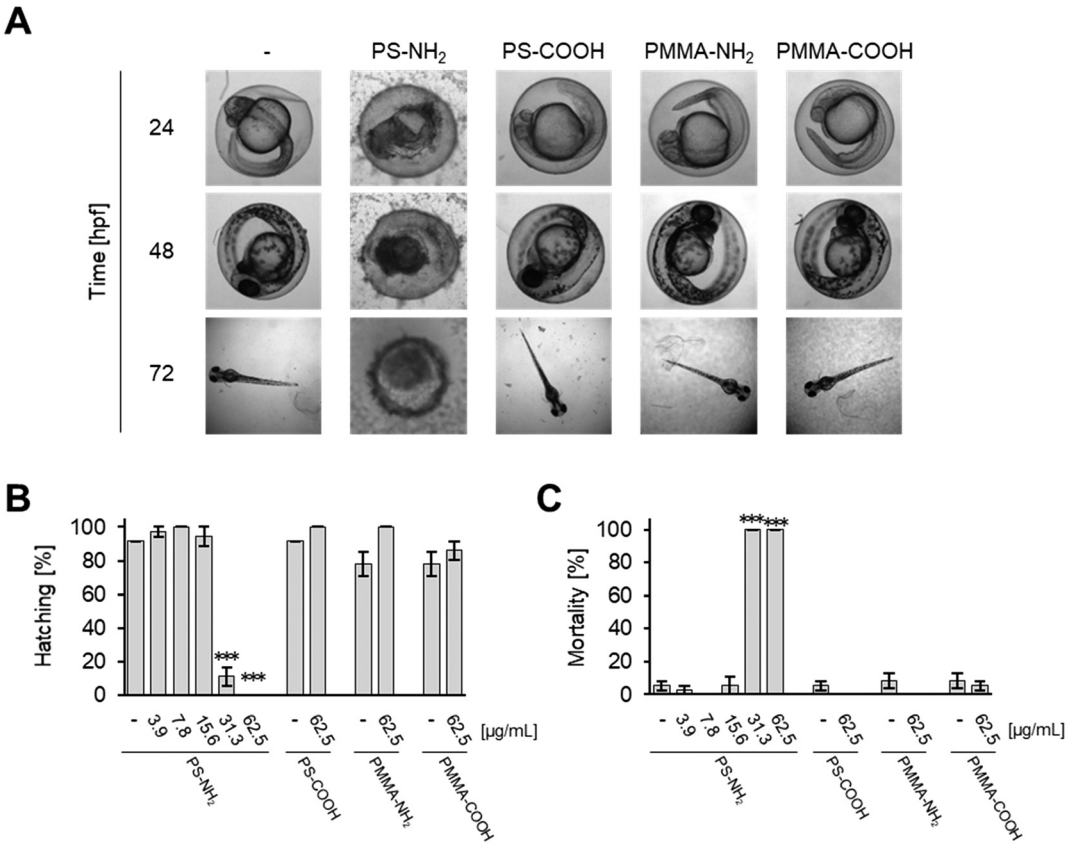

Fig. 5 Nanoplastics are toxic to zebrafish embryos dependent on surface modification and core chemistry. (A) PS-NH_2 but not PS-COOH, PMMA-NH_2, or PMMA-COOH NPs induce malformations and early mortality. Zebrafish embryos were exposed to 62.5 μg mL^{-1} NPs at 6 hpf and imaged at the indicated time points. Controls were exposed to Holtfreter's medium only (—). (B and C) PS-NH_2 but not PS-COOH, PMMA-NH_2 or PMMA-COOH provoke toxicity in zebrafish embryos. Hatching and mortality, normalised to the total number of analysed embryos, after 72 hpf are shown as a function of exposure concentration. Results shown are the means of 3 independent experiments ± s.e.m. (***$p < 0.001$).

Low toxicity MNMs

All SiO_2, TiO_2, and CeO_2 NPs, independent of their surface modification or different synthesis routes, appeared to show no toxicity in this study, as they did not induce a delay in hatching, malformations, or an increased mortality rate. A possible explanation is that the chorion protected the embryos from these poorly soluble MNMs, which could not pass through the chorion pores as either the size of the primary particles (in the case of silica) or of the agglomerates (in case of titania and ceria) is too big. In our studies, peak area intensity analysis indicated that 100% of the titania and ceria NPs are agglomerated. Particle agglomeration leads to sedimentation of larger particle agglomerates, thereby reducing the available fraction of non-agglomerated primary particles, which can move by diffusion to interact with the chorion. Therefore, zebrafish embryos might be protected from adverse effects of poorly soluble MNMs until hatching. This hypothesis could be tested in future experiments on embryos with and without the chorion and for different windows of exposure. The first days in zebrafish development are important for muscle and nerve formation and other organogenesis processes, which offer various possibilities for damage. In this sensitive period, small alterations can lead to malformations or death of the embryo. Therefore, the younger the embryos the higher their susceptibility might be for hazardous substances, and the greater the resulting damage.[91] With development proceeding towards their normal hatching time point, the embryos seem to be increasingly better prepared for resisting impacts from toxic substances in the water. Indeed, also after hatching embryos were not susceptible to SiO_2, TiO_2, and CeO_2 MNMs and could develop normally.

Due to their extensive use in cosmetics and paints, SiO_2 NPs can get into surface water and encounter aquatic organisms. Fent *et al.* detected no influence on hatching, development or mortality of zebrafish embryos exposed to low concentrations of fluorescently labelled amino-modified amorphous 60 nm and 200 nm SiO_2 NPs (0.0025, 0.25 and 25 μg mL^{-1}) until 96 hpf,[17] which supports the findings of our study. In contrast, Duan *et al.* found significantly increased mortality (22%) of zebrafish embryos exposed to amorphous 62 ± 7 nm SiO_2 NPs at higher concentrations (25, 50, 75, 100 and 200 μg mL^{-1}) at 96 hpf.[35,36] These authors also documented cardiovascular effects as well as oedema and bent tails at lower doses. The discrepant findings might be

explained by a different surface chemistry or synthesis route of the silica NPs (oil–water microemulsion core–shell particles in the first case *versus* Stöber synthesis in the latter).

In previous studies TiO_2 NPs (21 nm, anatase/rutile 3 : 1) were found to be non-toxic to zebrafish embryos and were therefore used as negative control in nanotoxicity experiments.[92] Our experiments also indicated no increase in embryo mortality or any effect on hatching and development up to 120 hpf upon exposure to different TiO_2 NPs at concentrations of 1 and 125 μg mL^{-1}, which may be related to the agglomerated state of the particles in the embryo medium leading to limited interaction. There are also studies in which toxicity due to TiO_2 NP (20–70 nm, anatase) exposure was observed at high concentrations (124.5 μg mL^{-1}).[93] As already outlined in the introduction, different TiO_2 NPs (21 nm, anatase/rutile 3 : 1, and 5–10 nm, anatase, respectively) in the presence of light induced malformation and mortality in zebrafish embryos.[16,39] In the latter studies, uptake of NPs into the larvae could be demonstrated by inductively coupled plasma optical emission spectrometry and transmission electron microscopy. Further, the findings suggest that embryos are protected by the chorion which interfered with NP uptake. Previous studies by Yang *et al.*[94] tested the effect of humic acid coating on TiO_2 NP (21 nm, anatase/rutile 3 : 1) toxicity. The adsorbed organic material increased the toxicity of TiO_2 NPs to zebrafish embryos in the absence and even more in the presence of light. A potential mechanism for the enhanced toxicity of TiO_2 NPs coated by humic acids seems to be related to an increase in oxidative DNA damage and subsequent cell death, possibly a result of improved dispersion of the particles and thus increased exposure. The latter exposure scenario is so far the one most closely mimicking the naturally occurring conditions.

In contrast to TiO_2 NPs, some CeO_2 NPs scavenge ROS and thereby enhance cell survival.[95] Antioxidant properties of protein-coated CeO_2 NPs were also demonstrated in zebrafish embryos, which prevented H_2O_2-induced oxidative stress, malformations, and death by abatement of intracellular ROS.[96] CeO_2 NPs were found to be non-toxic to zebrafish embryos in several studies,[41–43] which was confirmed by the results of this study. However, the influence of shape on CeO_2 NP toxicity has also been investigated, suggesting that, in contrast to the spherical CeO_2 NPs used in most studies, rod-like CeO_2 NPs trigger toxicity in the gut.[44]

Higher toxicity MNMs

Ag and ZnO NPs, at exposure concentrations exceeding predicted environmental concentrations,[10] were the most toxic NPs in our studies, presumably due to their solubility and the subsequent release of toxic metal ions.[79] The ecotoxicological endpoints hatching, malformation, and mortality were analysed. Whether these different phenotypes are mechanistically linked to each other, however, needs to be examined case by case. An embryo that fails to hatch will not be able to feed, is more susceptible to predators and has poor chances to survive. Reduced hatching rates in response to increasing NP concentrations could be a consequence of delayed development or death of the embryos. Another possibility is that the zebrafish hatching enzyme (ZHE1) is inhibited by metal ions that were released from the particles. This has been previously shown for Zn, Ni, and Cu ions,[33] and has been suggested for Ag ions.[28,97] It has further been proposed that the observed inhibition of hatching arose from the NPs themselves and not their dissolved metal components.[98] Such inhibition could potentially be a result of the NP adhesion to the chorion (as evidenced by the significant discolouration noted above), which may prevent light reaching the developing embryo, suggesting that an indirect effect at high NP concentrations could also contribute to the diminished hatching.[99,100] Mechanistically, light entrainment of the circadian clock controls hatching indirectly, possibly due to effects on the motility of the embryo, but also directly by its impact on the dopaminergic system, which regulates the release of the hatching enzyme.[99,100] Adhesion of PS-NPs (100 nm) to the chorion caused a hypoxic microenvironment and delayed hatching, although the chorion serves as a proper barrier for particle uptake.[101] This adverse effect might also be relevant for other MNMs adhering to the chorion and needs further study.

In our experiments, ZnO NPs were less potent in inhibiting hatching than soluble $ZnCl_2$ at equimolar Zn concentrations. This is in accordance with another study highlighting the critical role of soluble or free Zn^{2+} ions[79] in blocking the hatching of zebrafish embryos. Of note, inhibition of hatching by ZnO NPs was the most sensitive endpoint of those evaluated herein, and was observed already at 1 μg mL^{-1}, whereas no malformations and mortality occurred up to the highest tested dose of 125 μg mL^{-1}. Therefore, interference with hatching due to ZnO NPs or $ZnCl_2$ does not directly lead to malformations and mortality, indicating that these processes can be uncoupled and are independent events. However, a slight reduction in body length (8–10%) could be observed upon exposure to ZnO NPs in unhatched larvae at 5 dpf, suggesting that hatching inhibition might delay or inhibit development. Similarly, exposure to the same Ag NPs as used in our studies for 6 dpf reduced the body length in surviving larvae about 10% compared to unexposed controls.[6] In the case of hatching inhibition by Ag NPs, malformations and mortality followed a similar dose–response. Therefore, upon Ag NP exposure reduced hatching also could be a consequence of disturbed development or death of the embryos. Detrimental effects on survival and development by exposure to $AgNO_3$ were observed already at 10-fold lower concentrations, indicative of an essential role of Ag^+ ions in toxicity.[6]

Interestingly, we noticed a strong toxicity of specific nanoplastics, *i.e.*, PS-NH_2 NPs. Such a high toxicity of PS NPs to zebrafish embryos and larvae has not been documented before, since only non-functionalised PS NPs were investigated.[55] A number of reports found some adverse effects induced by plain polystyrene particles. However, acute

toxicity especially to zebrafish embryos is rather modest. In our studies, toxicity of PS NPs is dependent on surface functionalisation. As in the case of mammalian cells, amino-modified PS NPs but not carboxylated PS NPs are toxic to early embryonic stages. Although carboxylated PS NPs seem not to induce acute toxic effects, a number of other adverse effects, such as deregulation of intestinal iron uptake or activation of ion channels, have been reported[102] and warrant further investigations. Our findings in zebrafish embryos are reminiscent of similar results obtained with sea urchin embryos,[103–105] where amino-modified PS NPs are toxic and carboxylation of PS NPs can render these materials biocompatible. These observations provide a clue for a safe-by-design approach to circumvent deleterious effects on vulnerable aquatic organisms. Importantly, not only the amino-groups at the surface of nanoplastics determines their toxicity but also the core chemistry. In our hands, amino-modified PMMA NPs, with a similar degree of amine functionalisation as that on the PS-NH_2 NPs, were non-toxic to zebrafish embryos up to 5 dpf regarding the acute endpoints hatching, malformations, and survival, indicating that simply considering surface groups is not sufficient to predict toxicity. However, this does not indicate that PMMA NPs are in general non-toxic. In a recent study in fish (juvenile sea bass), exposure to PMMA NPs (around 50 nm) altered gene expression related to lipid metabolism.[106] For fluorescently labelled PMMA NPs, uptake by aquatic organisms such as barnacles[107] and water fleas[108] has been demonstrated. At present, we can only speculate on the different toxicity of amino-modified PS and PMMA NPs. For example, different linker lengths to couple the amino-groups to the surface and regional differences in the density of such functional groups on the particle surface might alter interactions at the nano-biointerface. Furthermore, the polymer chemistry (such as PMMA *versus* PS) might as well affect the reactivity of the amino-groups at the surface. Clearly, further research is needed to more precisely characterise the importance of surface chemistry of nanoplastics composed of different polymers to establish structure–activity relationships with a potential to support the safe-by-design concept.

A further challenge in the safety assessment of nanoplastics relates to the difficulties to unambiguously detect nanoplastics at high resolution and at the single particle level in biological tissues. For non-labelled nanoplastics found in the environment with rather heterogenous shapes and sizes, detection in tissues will remain difficult if not impossible. In our studies engineered, monodisperse polystyrene NPs were used which, due to their homogeneous spherical shape and size, could be specifically identified outside of cells, *e.g.*, attached to the chorion, by TEM. However, inside of cells, carbon-based nanomaterials are hard to distinguish, as the atomic number does not differ from that of the biological matrix. For synthesized model nanoplastics intended for experimental studies, heavy elements such as metals could be incorporated which can facilitate quantification of particles by mass spectrometry in environmental samples such as activated sludge,[109] but could potentially be also suited to enable identification by transmission electron microscopy in biological specimen.[110,111]

Summary and conclusions

In an interdisciplinary approach, a well characterized library of MNMs with distinct physico-chemical properties was assessed for their potential induction of adverse effects in zebrafish embryos. Building on our experience with this MNM library and their impact on mammalian cells, we now investigated potential toxicity in an entire organism focusing on lethality, effects on development, and hatching. Through our systematic analysis employing high-throughput imaging we highlight the relevance of material chemistry but also surface functionalisation as key parameters to be considered for future MNM safe-by design strategies. These principles are also of specific relevance for the assessment of emerging micropollutants such as nanoplastics. As imaging-based high throughput screening to assess adverse effects of MNMs in zebrafish has not been frequently used so far in the field, some future research and developments also are suggested. Whereas embryos within the chorion already can be efficiently imaged and analysed by dedicated software, for hatched larvae this is not so simple. Novel technologies and software solutions, such as machine learning approaches for image analysis, are motivated by our findings in order to further establish high-throughput imaging of zebrafish larvae as a powerful and promising tool for hazard assessment of MNMs, but also of chemicals in general.

Author contributions

Conceptualization and supervision: I. L., E. V.-J., S. D., C. W.; zebrafish screens: I. H., J. R., L. R., D. M., S. A., C. A., G. P., R. P., S. R.; transmission electron microscopy and histology: M. T., S. A.; NP synthesis and characterization: S. F.-D., I.-L. H., D. G., I. O.-J., S. V. Y. A., M. F. A. B. D. N., A. O. K.; original draft preparation: S. D., S. F.-D., M. T., C. W.; review and editing: T. D., S. R., S. F.-D., I. L., E. V.-J., C. W.; project administration and funding acquisition: S. D., I. L., E. V.-J., U. S., C. W.

Conflicts of interest

The authors declare that they have no conflict of interest.

Acknowledgements

This research was funded by the European Commission's 7th Framework Program (FP7/2007-2013) research project NanoMILE (Contract No. NMP4-LA-2013-310451). We thank Nicholas Foulkes for helpful comments on the manuscript and Katrin Volkmann for technical assistance.

References

1 S. Lin, Y. Zhao, A. E. Nel and S. Lin, Zebrafish: an in vivo model for nano EHS studies, *Small*, 2013, **9**, 1608–1618.

2 U. Strähle, S. Scholz, R. Geisler, P. Greiner, H. Hollert, S. Rastegar, A. Schumacher, I. Selderslaghs, C. Weiss, H. Witters and T. Braunbeck, Zebrafish embryos as an alternative to animal experiments–a commentary on the definition of the onset of protected life stages in animal welfare regulations, *Reprod. Toxicol.*, 2012, **33**, 128–132.

3 L. Yang, N. Y. Ho, R. Alshut, J. Legradi, C. Weiss, M. Reischl, R. Mikut, U. Liebel, F. Müller and U. Strähle, Zebrafish embryos as models for embryotoxic and teratological effects of chemicals, *Reprod. Toxicol.*, 2009, **28**, 245–253.

4 K. Howe, M. D. Clark, C. F. Torroja, J. Torrance, C. Berthelot, M. Muffato, J. E. Collins, S. Humphray, K. McLaren, L. Matthews, S. McLaren, I. Sealy, M. Caccamo, C. Churcher, C. Scott, J. C. Barrett, R. Koch, G.-J. Rauch, S. White, W. Chow, B. Kilian, L. T. Quintais, J. A. Guerra-Assunção, Y. Zhou, Y. Gu, J. Yen, J.-H. Vogel, T. Eyre, S. Redmond, R. Banerjee, J. Chi, B. Fu, E. Langley, S. F. Maguire, G. K. Laird, D. Lloyd, E. Kenyon, S. Donaldson, H. Sehra, J. Almeida-King, J. Loveland, S. Trevanion, M. Jones, M. Quail, D. Willey, A. Hunt, J. Burton, S. Sims, K. McLay, B. Plumb, J. Davis, C. Clee, K. Oliver, R. Clark, C. Riddle, D. Elliott, G. Threadgold, G. Harden, D. Ware, S. Begum, B. Mortimore, G. Kerry, P. Heath, B. Phillimore, A. Tracey, N. Corby, M. Dunn, C. Johnson, J. Wood, S. Clark, S. Pelan, G. Griffiths, M. Smith, R. Glithero, P. Howden, N. Barker, C. Lloyd, C. Stevens, J. Harley, K. Holt, G. Panagiotidis, J. Lovell, H. Beasley, C. Henderson, D. Gordon, K. Auger, D. Wright, J. Collins, C. Raisen, L. Dyer, K. Leung, L. Robertson, K. Ambridge, D. Leongamornlert, S. McGuire, R. Gilderthorp, C. Griffiths, D. Manthravadi, S. Nichol, G. Barker, S. Whitehead, M. Kay, J. Brown, C. Murnane, E. Gray, M. Humphries, N. Sycamore, D. Barker, D. Saunders, J. Wallis, A. Babbage, S. Hammond, M. Mashreghi-Mohammadi, L. Barr, S. Martin, P. Wray, A. Ellington, N. Matthews, M. Ellwood, R. Woodmansey, G. Clark, J. D. Cooper, A. Tromans, D. Grafham, C. Skuce, R. Pandian, R. Andrews, E. Harrison, A. Kimberley, J. Garnett, N. Fosker, R. Hall, P. Garner, D. Kelly, C. Bird, S. Palmer, I. Gehring, A. Berger, C. M. Dooley, Z. Ersan-Ürün, C. Eser, H. Geiger, M. Geisler, L. Karotki, A. Kirn, J. Konantz, M. Konantz, M. Oberländer, S. Rudolph-Geiger, M. Teucke, C. Lanz, G. Raddatz, K. Osoegawa, B. Zhu, A. Rapp, S. Widaa, C. Langford, F. Yang, S. C. Schuster, N. P. Carter, J. Harrow, Z. Ning, J. Herrero, S. M. J. Searle, A. Enright, R. Geisler, R. H. A. Plasterk, C. Lee, M. Westerfield, P. J. de Jong, L. I. Zon, J. H. Postlethwait, C. Nüsslein-Volhard, T. J. P. Hubbard, H. R. Crollius, J. Rogers and D. L. Stemple, The zebrafish reference genome sequence and its relationship to the human genome, *Nature*, 2013, **496**, 498–503.

5 OECD, *OECD 236 - Guideline for the testing of chemicals: fish embryo acute toxicity (FET) test*, 2013.

6 B. J. Shaw, C. C. Liddle, K. M. Windeatt and R. D. Handy, A critical evaluation of the fish early-life stage toxicity test for engineered nanomaterials: experimental modifications and recommendations, *Arch. Toxicol.*, 2016, **90**, 2077–2107.

7 OECD, *Series on the safety of manufactured nanomaterials No. 27. List of manufactured nanomaterials and list of endpoints for phase one of the sponsorship programme for the testing of manufactured nanomaterials: revision*, Organization for Economic Co-operation and Development (OECD), Environment directorate, Paris, 2010.

8 R. D. Handy, T. B. Henry, T. M. Scown, B. D. Johnston and C. R. Tyler, Manufactured nanoparticles: their uptake and effects on fish–a mechanistic analysis, *Ecotoxicology*, 2008, **17**, 396–409.

9 R. D. Handy, K. F. von der, J. R. Lead, M. Hassellov, R. Owen and M. Crane, The ecotoxicology and chemistry of manufactured nanoparticles, *Ecotoxicology*, 2008, **17**, 287–314.

10 F. Gottschalk, T. Sonderer, R. W. Scholz and B. Nowack, Modeled Environmental Concentrations of Engineered Nanomaterials (TiO2, ZnO, Ag, CNT, Fullerenes) for Different Regions, *Environ. Sci. Technol.*, 2009, **43**, 9216–9222.

11 I. Hansjosten, J. Rapp, L. Reiner, R. Vatter, S. Fritsch-Decker, R. Peravali, T. Palosaari, E. Joossens, K. Gerloff, P. Macko, M. Whelan, D. Gilliland, I. Ojea-Jimenez, M. P. Monopoli, L. Rocks, D. Garry, K. Dawson, P. J. F. Röttgermann, A. Murschhauser, J. O. Rädler, S. V. Y. Tang, P. Gooden, M. A. Belinga-Desaunay, A. O. Khan, S. Briffa, E. Guggenheim, A. Papadiamantis, I. Lynch, E. Valsami-Jones, S. Diabaté and C. Weiss, Microscopy-based high-throughput assays enable multi-parametric analysis to assess adverse effects of nanomaterials in various cell lines, *Arch. Toxicol.*, 2018, **92**, 633–649.

12 S. Anguissola, D. Garry, A. Salvati, P. J. O'Brien and K. A. Dawson, High content analysis provides mechanistic insights on the pathways of toxicity induced by amine-modified polystyrene nanoparticles, *PLoS One*, 2014, **9**, e108025.

13 T. Xia, M. Kovochich, M. Liong, J. I. Zink and A. E. Nel, Cationic polystyrene nanosphere toxicity depends on cell-specific endocytic and mitochondrial injury pathways, *ACS Nano*, 2008, **2**, 85–96.

14 D. M. Rawson, T. Zhang, D. Kalicharian and W. L. Jongebloed, Field emission scanning electron microscopy and transmission electron microscopy studies of the chorion, plasma membrane and syncytial layers of the gastrula-stage embryo of the zebrafish *Brachydanio rerio*: a consideration of the structural and functional relationships with respect to cytoprotectant penetration, *Aquacult. Res.*, 2000, **31**, 325–336.

15 B. Kais, K. E. Schneider, S. Keiter, K. Henn, C. Ackermann and T. Braunbeck, DMSO modifies the permeability of the zebrafish (Danio rerio) chorion-implications for the fish embryo test (FET), *Aquat. Toxicol.*, 2013, **140–141**, 229–238.

16 O. Bar-Ilan, K. M. Louis, S. P. Yang, J. A. Pedersen, R. J. Hamers, R. E. Peterson and W. Heideman, Titanium dioxide nanoparticles produce phototoxicity in the developing zebrafish, *Nanotoxicology*, 2012, **6**, 670–679.

17 K. Fent, C. J. Weisbrod, A. Wirth-Heller and U. Pieles, Assessment of uptake and toxicity of fluorescent silica nanoparticles in zebrafish (Danio rerio) early life stages, *Aquat. Toxicol.*, 2010, **100**, 218–228.

18 K. J. Lee, L. M. Browning, P. D. Nallathamby, T. Desai, P. K. Cherukuri and X. H. Xu, In vivo quantitative study of sized-dependent transport and toxicity of single silver nanoparticles using zebrafish embryos, *Chem. Res. Toxicol.*, 2012, **25**, 1029–1046.

19 S. George, T. Xia, R. Rallo, Y. Zhao, Z. Ji, S. Lin, X. Wang, H. Zhang, B. France, D. Schoenfeld, R. Damoiseaux, R. Liu, S. Lin, K. A. Bradley, Y. Cohen and A. E. Nel, Use of a high-throughput screening approach coupled with in vivo zebrafish embryo screening to develop hazard ranking for engineered nanomaterials, *ACS Nano*, 2011, **5**, 1805–1817.

20 B. J. Shaw and R. D. Handy, Physiological effects of nanoparticles on fish: a comparison of nanometals versus metal ions, *Environ. Int.*, 2011, **37**, 1083–1097.

21 H. J. Johnston, G. Hutchison, F. M. Christensen, S. Peters, S. Hankin and V. Stone, A review of the in vivo and in vitro toxicity of silver and gold particulates: particle attributes and biological mechanisms responsible for the observed toxicity, *Crit. Rev. Toxicol.*, 2010, **40**, 328–346.

22 B. Reidy, A. Haase, A. Luch, K. A. Dawson and I. Lynch, Mechanisms of silver nanoparticle release, transformation and toxicity: a critical review of current knowledge and recommendations for future studies and applications, *Materials*, 2013, **6**, 2295–2350.

23 J. Fabrega, S. N. Luoma, C. R. Tyler, T. S. Galloway and J. R. Lead, Silver nanoparticles: behaviour and effects in the aquatic environment, *Environ. Int.*, 2011, **37**, 517–531.

24 L.-J. A. Ellis, S. Kissane, E. Hoffman, J. B. Brown, E. Valsami-Jones, J. Colbourne and I. Lynch, Multigenerational Exposures of Daphnia Magna to Pristine and Aged Silver Nanoparticles: Epigenetic Changes and Phenotypical Ageing Related Effects, *Small*, 2020, **16**, 2000301.

25 C. M. Powers, T. A. Slotkin, F. J. Seidler, A. R. Badireddy and S. Padilla, Silver nanoparticles alter zebrafish development and larval behavior: distinct roles for particle size, coating and composition, *Neurotoxicol. Teratol.*, 2011, **33**, 708–714.

26 S. George, S. Lin, Z. Ji, C. R. Thomas, L. Li, M. Mecklenburg, H. Meng, X. Wang, H. Zhang, T. Xia, J. N. Hohman, S. Lin, J. I. Zink, P. S. Weiss and A. E. Nel, Surface defects on plate-shaped silver nanoparticles contribute to its hazard potential in a fish gill cell line and zebrafish embryos, *ACS Nano*, 2012, **6**, 3745–3759.

27 O. J. Osborne, K. Mukaigasa, H. Nakajima, B. Stolpe, I. Romer, U. Philips, I. Lynch, S. Mourabit, S. Hirose, J. R. Lead, M. Kobayashi, T. Kudoh and C. R. Tyler, Sensory systems and ionocytes are targets for silver nanoparticle effects in fish, *Nanotoxicology*, 2016, **10**, 1276–1286.

28 A. Massarsky, L. Dupuis, J. Taylor, S. Eisa-Beygi, L. Strek, V. L. Trudeau and T. W. Moon, Assessment of nanosilver toxicity during zebrafish (Danio rerio) development, *Chemosphere*, 2013, **92**, 59–66.

29 O. J. Osborne, B. D. Johnston, J. Moger, M. Balousha, J. R. Lead, T. Kudoh and C. R. Tyler, Effects of particle size and coating on nanoscale Ag and TiO_2 exposure in zebrafish (Danio rerio) embryos, *Nanotoxicology*, 2013, **7**(8), 1315–1324.

30 Q. Mu, C. A. David, J. Galceran, C. Rey-Castro, L. Krzeminski, R. Wallace, F. Bamiduro, S. J. Milne, N. S. Hondow, R. Brydson, G. Vizcay-Barrena, M. N. Routledge, L. J. Jeuken and A. P. Brown, Systematic investigation of the physicochemical factors that contribute to the toxicity of ZnO nanoparticles, *Chem. Res. Toxicol.*, 2014, **27**, 558–567.

31 W. Wu, P. A. Bromberg and J. M. Samet, Zinc ions as effectors of environmental oxidative lung injury, *Free Radical Biol. Med.*, 2013, **65**, 57–69.

32 W. S. Cho, R. Duffin, S. E. Howie, C. J. Scotton, W. A. Wallace, W. MacNee, M. Bradley, I. L. Megson and K. Donaldson, Progressive severe lung injury by zinc oxide nanoparticles; the role of Zn2+ dissolution inside lysosomes, *Part. Fibre Toxicol.*, 2011, **8**, 27.

33 S. Lin, Y. Zhao, Z. Ji, J. Ear, C. H. Chang, H. Zhang, C. Low-Kam, K. Yamada, H. Meng, X. Wang, R. Liu, S. Pokhrel, L. Mädler, R. Damoiseaux, T. Xia, H. A. Godwin, S. Lin and A. E. Nel, Zebrafish high-throughput screening to study the impact of dissolvable metal oxide nanoparticles on the hatching enzyme, ZHE1, *Small*, 2013, **9**, 1776–1785.

34 X. Zhao, S. Wang, Y. Wu, H. You and L. Lv, Acute ZnO nanoparticles exposure induces developmental toxicity, oxidative stress and DNA damage in embryo-larval zebrafish, *Aquat. Toxicol.*, 2013, **136–137**, 49–59.

35 J. Duan, Y. Yu, Y. Li, Y. Yu and Z. Sun, Cardiovascular toxicity evaluation of silica nanoparticles in endothelial cells and zebrafish model, *Biomaterials*, 2013, **34**, 5853–5862.

36 J. Duan, Y. Yu, H. Shi, L. Tian, C. Guo, P. Huang, X. Zhou, S. Peng and Z. Sun, Toxic effects of silica nanoparticles on zebrafish embryos and larvae, *PLoS One*, 2013, **8**, e74606.

37 C. Pavan, R. Santalucia, R. Leinardi, M. Fabbiani, Y. Yakoub, F. Uwambayinema, P. Ugliengo, M. Tomatis, G. Martra, F. Turci, D. Lison and B. Fubini, Nearly free surface silanols are the critical molecular moieties that initiate the toxicity of silica particles, *Proc. Natl. Acad. Sci. U. S. A.*, 2020, **117**, 27836–27846.

38 C. Pavan, M. Delle Piane, M. Gullo, F. Filippi, B. Fubini, P. Hoet, C. J. Horwell, F. Huaux, D. Lison, C. Lo Giudice, G. Martra, E. Montfort, R. Schins, M. Sulpizi, K. Wegner, M. Wyart-Remy, C. Ziemann and F. Turci, The puzzling issue of silica toxicity: are silanols bridging the gaps between surface states and pathogenicity?, *Part. Fibre Toxicol.*, 2019, **16**, 32.

39 O. Bar-Ilan, C. C. Chuang, D. J. Schwahn, S. Yang, S. Joshi, J. A. Pedersen, R. J. Hamers, R. E. Peterson and W. Heideman, TiO2 nanoparticle exposure and illumination during zebrafish development: mortality at parts per billion concentrations, *Environ. Sci. Technol.*, 2013, **47**(9), 4726–4733.

40 M. Faria, J. M. Navas, D. Raldua, A. M. Soares and C. Barata, Oxidative stress effects of titanium dioxide nanoparticle aggregates in zebrafish embryos, *Sci. Total Environ.*, 2014, **470–471**, 379–389.

41 K. Van Hoecke, J. T. Quik, J. Mankiewicz-Boczek, K. A. De Schamphelaere, A. Elsaesser, P. Van der Meeren, C. Barnes, G. McKerr, C. V. Howard, D. Van de Meent, K. Rydzynski, K. A. Dawson, A. Salvati, A. Lesniak, I. Lynch, G. Silversmit, S. B. De, L. Vincze and C. R. Janssen, Fate and effects of CeO2 nanoparticles in aquatic ecotoxicity tests, *Environ. Sci. Technol.*, 2009, **43**, 4537–4546.

42 A. Jemec, P. Djinovic, T. Tisler and A. Pintar, Effects of four CeO2 nanocrystalline catalysts on early-life stages of zebrafish Danio rerio and crustacean Daphnia magna, *J. Hazard. Mater.*, 2012, **219–220**, 213–220.

43 A. Jemec, P. Djinovic, I. G. Crnivec and A. Pintar, The hazard assessment of nanostructured CeO(2)-based mixed oxides on the zebrafish Danio rerio under environmentally relevant UV-A exposure, *Sci. Total Environ.*, 2015, **506–507**, 272–278.

44 S. Lin, X. Wang, Z. Ji, C. H. Chang, Y. Dong, H. Meng, Y. P. Liao, M. Wang, T. B. Song, S. Kohan, T. Xia, J. I. Zink, S. Lin and A. E. Nel, Aspect ratio plays a role in the hazard potential of CeO2 nanoparticles in mouse lung and zebrafish gastrointestinal tract, *ACS Nano*, 2014, **8**, 4450–4464.

45 M. Cole, P. Lindeque, E. Fileman, C. Halsband, R. Goodhead, J. Moger and T. S. Galloway, Microplastic ingestion by zooplankton, *Environ. Sci. Technol.*, 2013, **47**, 6646–6655.

46 J. Hammer, M. H. Kraak and J. R. Parsons, Plastics in the marine environment: the dark side of a modern gift, *Rev. Environ. Contam. Toxicol.*, 2012, **220**, 1–44.

47 S. Krause, V. Baranov, H. A. Nel, J. D. Drummond, A. Kukkola, T. Hoellein, G. H. Sambrook Smith, J. Lewandowski, B. Bonet, A. I. Packman, J. Sadler, V. Inshyna, S. Allen, D. Allen, L. Simon, F. Mermillod-Blondin and I. Lynch, Gathering at the top? Environmental controls of microplastic uptake and biomagnification in freshwater food webs, *Environ. Pollut.*, 2021, **268**, 115750.

48 E. Besseling, P. Redondo-Hasselerharm, E. M. Foekema and A. A. Koelmans, Quantifying ecological risks of aquatic micro- and nanoplastic, *Crit. Rev. Environ. Sci. Technol.*, 2019, **49**, 32–80.

49 A. A. Koelmans, E. Besseling, W. J. Shim and M. Bergmann, in *Marine anthropogenic litter*, ed. M. Bergmann, L. Gutow and M. Klages, Springer, Cham, Heidelberg, New York, Dordrecht, London, 2015, pp. 325–340.

50 R. Triebskorn, T. Braunbeck, T. Grummt, L. Hanslik, S. Huppertsberg, M. Jekel, T. P. Knepper, S. Krais, Y. K. Muller, M. Pittroff, A. S. Ruhl, H. Schmieg, C. Schur, C. Strobel, M. Wagner, N. Zumbulte and H. R. Kohler, Relevance of nano- and microplastics for freshwater ecosystems: A critical review, *TrAC, Trends Anal. Chem.*, 2019, **110**, 375–392.

51 S. Kashiwada, Distribution of nanoparticles in the see-through medaka (Oryzias latipes), *Environ. Health Perspect.*, 2006, **114**, 1697–1702.

52 K. Mattsson, M. T. Ekvall, L. A. Hansson, S. Linse, A. Malmendal and T. Cedervall, Altered behavior, physiology, and metabolism in fish exposed to polystyrene nanoparticles, *Environ. Sci. Technol.*, 2015, **49**, 553–561.

53 K. Mattsson, E. V. Johnson, A. Malmendal, S. Linse, L. A. Hansson and T. Cedervall, Brain damage and behavioural disorders in fish induced by plastic nanoparticles delivered through the food chain, *Sci. Rep.*, 2017, **7**, 11452.

54 J. A. Pitt, J. S. Kozal, N. Jayasundara, A. Massarsky, R. Trevisan, N. Geitner, M. Wiesner, E. D. Levin and R. T. Di Giulio, Uptake, tissue distribution, and toxicity of polystyrene nanoparticles in developing zebrafish (Danio rerio), *Aquat. Toxicol.*, 2018, **194**, 185–194.

55 J. Bhagat, L. Zang, N. Nishimura and Y. Shimada, Zebrafish: An emerging model to study microplastic and nanoplastic toxicity, *Sci. Total Environ.*, 2020, **728**, 138707.

56 Y. Y. Zhang and G. G. Goss, Potentiation of polycyclic aromatic hydrocarbon uptake in zebrafish embryos by nanoplastics, *Environ. Sci.: Nano*, 2020, **7**, 1730–1741.

57 Q. Chen, D. Yin, Y. Jia, S. Schiwy, J. Legradi, S. Yang and H. Hollert, Enhanced uptake of BPA in the presence of nanoplastics can lead to neurotoxic effects in adult zebrafish, *Sci. Total Environ.*, 2017, **609**, 1312–1321.

58 M. Sendra, P. Pereiro, M. P. Yeste, L. Mercado, A. Figueras and B. Novoa, Size matters: Zebrafish (Danio rerio) as a model to study toxicity of nanoplastics from cells to the whole organism, *Environ. Pollut.*, 2020, **268**, 115769.

59 L. Landgraf, D. Nordmeyer, P. Schmiel, Q. Gao, S. Ritz, S. Gebauer, S. Graß, S. Diabaté, L. Treuel, C. Graf, E. Rühl, K. Landfester, V. Mailänder, C. Weiss, R. Zellner and I. Hilger, Validation of weak biological effects by round robin experiments: cytotoxicity/biocompatibility of SiO2 and polymer nanoparticles in HepG2 cells, *Sci. Rep.*, 2017, **7**, 4341.

60 S. R. Mane, I. L. Hsiao, M. Takamiya, D. Le, U. Straehle, C. Barner-Kowollik, C. Weiss and G. Delaittre, Intrinsically fluorescent, stealth polypyrazoline nanoparticles with large stokes shift for in vivo imaging, *Small*, 2018, **14**, e1801571.

61 R. Alshut, J. Legradi, U. Liebel, L. Yang, J. van Wezel, U. Strähle, R. Mikut and M. Reischl, Methods for automated high-throughput toxicity testing using zebrafish embryos, *Lecture Notes in Artificial Intelligence*, 2010, vol. 6359, pp. 219–226.

62 K. Rasmussen, J. Mast, P. J. De Temmerman, E. Verleysen, N. Waegeneers, F. Van Steen, J. C. Pizzolon, L. De Temmerman, E. Van Doren, K. A. Jensen, R. Birkedal, M. Levin, S. H. Nielsen, I. K. Koponen, P. A. Clausen, V. Kofoed-Sorensen, Y. Kembouche, N. Thieriet, O. Spalla, C.

Guiot, D. Rousset, O. Witschger, S. Bau, B. Bianchi, C. Motzkus, B. Shivachev, L. Dimova, R. Nikolova, D. Nihtianova, M. Tarassov, O. Petrov, S. Bakardjieva, D. Gilliland, F. Pianella, G. Ceccone, V. Spampinato, G. Cotogno, N. Gibson, C. Gaillard and A. Mech, *Titanium dioxide, NM-100, NM-101, NM-102, NM-103, NM-104, NM-105: Characterisation and physico-chemical properties*, Publications Office of the European Union, Luxembourg, 2014.

63 C. Singh, S. Friedrichs, G. Ceccone, N. Gibson, K. A. Jensen, M. Levin, H. G. Infante, D. Carlander and K. Rasmussen, *Cerium dioxide, NM-211, NM-212, NM-213. Characterisation and test item preparation*, Publications Office of the European Union, Luxembourg, 2014.

64 C. Singh, S. Friedrichs, M. Levin, R. Birkedal, K. A. Jensen, G. Pojana, W. Wohlleben, S. Schulte, K. Wiench, T. Turney, O. Koulaeva, D. Marshall, K. Hund-Rinke, W. Kördel, E. Van Doren, P. J. De Temmermann, M. Abi Daoud Francisco, J. Mast, N. Gibson, R. Koeber, T. Linsinger and C. L. Klein, *Zinc oxide NM-110, NM-111, NM-112, NM-113. Characterisation and test item preparation*, Publications Office of the European Union, Luxembourg, 2011.

65 C. L. Klein, S. Comero, B. Stahlmecke, J. Romazanov, T. A. J. Kuhlbusch, E. Van Doren, P.-J. De Temmermann, J. Mast, P. Wick, H. Krug, G. Locoro, K. Hund-Rinke, W. Kördel, S. Friedrichs, G. Maier, J. Werner, T. Linsinger and B. M. Gawlik, *NM-300 silver. Characterisation, stability, homogeneity*, Publications Office of the European Union, Luxembourg, 2011.

66 E. Lester, P. Blood, J. Denyer, D. Giddings, B. Azzopardi and M. Poliakoff, Reaction engineering: The supercritical water hydrothermal synthesis of nano-particles, *J. Supercrit. Fluids*, 2006, **37**, 209–214.

67 E. Lester, S. V. Y. Tang, A. Khlobystov, V. L. Rose, L. Buttery and C. J. Roberts, Producing nanotubes of biocompatible hydroxyapatite by continuous hydrothermal synthesis, *CrystEngComm*, 2013, **15**, 3256–3260.

68 E. Joossens, P. Macko, T. Palosaari, K. Gerloff, I. Ojea-Jiménez, D. Gilliland, J. Novak, S. Fortaner Torrent, J.-M. Gineste, I. Römer, S. M. Briffa, E. Valsami-Jones, I. Lynch and M. Whelan, A high throughput imaging database of toxicological effects of nanomaterials tested on HepaRG cells, *Sci. Data*, 2019, **6**, 46.

69 A. O. Khan, A. Di Maio, E. J. Guggenheim, A. J. Chetwynd, D. Pencross, S. Tang, M.-F. A. Belinga-Desaunay, S. G. Thomas, J. Z. Rappoport and I. Lynch, Surface Chemistry-Dependent Evolution of the Nanomaterial Corona on TiO2 Nanomaterials Following Uptake and Sub-Cellular Localization, *Nanomaterials*, 2020, **10**, 401.

70 I. Ojea-Jimenez, P. Urban, F. Barahona, M. Pedroni, R. Capomaccio, G. Ceccone, A. Kinsner-Ovaskainen, F. Rossi and D. Gilliland, Highly flexible platform for tuning surface properties of silica nanoparticles and monitoring their biological interaction, *ACS Appl. Mater. Interfaces*, 2016, **8**, 4838–4850.

71 K. A. Jensen, Y. Kembouche, E. Christiansen, N. R. Jacobsen, H. Wallin, C. Guiot, O. Spalla and O. Witschger, *Final protocol for producing suitable manufactured nanomaterial exposure media - Standard Operation Procedure (SOP) and background documentation*, https://www.anses.fr/en/system/files/nanogenotox_deliverable_5.pdf, (accessed 04.08.2020).

72 C. Marquardt, S. Fritsch-Decker, M. Al-Rawi, S. Diabaté and C. Weiss, Autophagy induced by silica nanoparticles protects RAW264.7 macrophages from cell death, *Toxicology*, 2017, **379**, 40–47.

73 C. B. Kimmel, W. W. Ballard, S. R. Kimmel, B. Ullmann and T. F. Schilling, Stages of embryonic development of the zebrafish, *Dev. Dyn.*, 1995, **203**, 253–310.

74 M. Westerfield, *The Zebrafish Book*, University of Oregon Press, Eugene, OR, 1995.

75 P. Aleström, L. D'Angelo, P. J. Midtlyng, D. F. Schorderet, S. Schulte-Merker, F. Sohm and S. Warner, Zebrafish: Housing and husbandry recommendations, *Lab. Anim.*, 2020, **54**, 213–224.

76 M. Takamiya, J. Stegmaier, A. Y. Kobitski, B. Schott, B. D. Weger, D. Margariti, A. R. Cereceda Delgado, V. Gourain, T. Scherr, L. Yang, S. Sorge, J. C. Otte, V. Hartmann, J. van Wezel, R. Stotzka, T. Reinhard, G. Schlunck, T. Dickmeis, S. Rastegar, R. Mikut, G. U. Nienhaus and U. Strähle, Pax6 organizes the anterior eye segment by guiding two distinct neural crest waves, *PLoS Genet.*, 2020, **16**, e1008774.

77 I. L. Hsiao, S. Fritsch-Decker, A. Leidner, M. Al-Rawi, V. Hug, S. Diabaté, S. L. Grage, M. Meffert, T. Stoeger, D. Gerthsen, A. S. Ulrich, C. M. Niemeyer and C. Weiss, Biocompatibility of Amine-Functionalized Silica Nanoparticles: The Role of Surface Coverage, *Small*, 2019, e1805400, DOI: 10.1002/smll.201805400.

78 V. Y. A. Davydov, in *Adsorption on silica surfaces*, ed. E. Papirer, Marcel Dekker, Inc., New York, Basel, 2000, pp. 63–118.

79 N. R. Brun, M. Lenz, B. Wehrli and K. Fent, Comparative effects of zinc oxide nanoparticles and dissolved zinc on zebrafish embryos and eleuthero-embryos: importance of zinc ions, *Sci. Total Environ.*, 2014, **476–477**, 657–666.

80 N. Jeliazkova, M. D. Apostolova, C. Andreoli, F. Barone, A. Barrick, C. Battistelli, C. Bossa, A. Botea-Petcu, A. Châtel, I. De Angelis, M. Dusinska, N. El Yamani, D. Gheorghe, A. Giusti, P. Gómez-Fernández, R. Grafström, M. Gromelski, N. R. Jacobsen, V. Jeliazkov, K. A. Jensen, N. Kochev, P. Kohonen, N. Manier, E. Mariussen, A. Mech, J. M. Navas, V. Paskaleva, A. Precupas, T. Puzyn, K. Rasmussen, P. Ritchie, I. R. Llopis, E. Rundén-Pran, R. Sandu, N. Shandilya, S. Tanasescu, A. Haase and P. Nymark, Towards FAIR nanosafety data, *Nat. Nanotechnol.*, 2021, **16**, 644–654.

81 P. Karatzas, G. Melagraki, L.-J. A. Ellis, I. Lynch, D.-D. Varsou, A. Afantitis, A. Tsoumanis, P. Doganis and H. Sarimveis, Development of Deep Learning Models for Predicting the Effects of Exposure to Engineered Nanomaterials on Daphnia magna, *Small*, 2020, **16**, 2001080.

82 R. Mikut, T. Dickmeis, W. Driever, P. Geurts, F. A. Hamprecht, B. X. Kausler, M. J. Ledesma-Carbayo, R. Maree, K. Mikula, P. Pantazis, O. Ronneberger, A. Santos, R. Stotzka, U. Strahle and N. Peyrieras, Automated processing of zebrafish imaging data: a survey, *Zebrafish*, 2013, **10**, 401–421.

83 R. Liu, S. Lin, R. Rallo, Y. Zhao, R. Damoiseaux, T. Xia, S. Lin, A. Nel and Y. Cohen, Automated phenotype recognition for zebrafish embryo based in vivo high throughput toxicity screening of engineered nano-materials, *PLoS One*, 2012, **7**, e35014.

84 J. Gehrig, M. Reischl, E. Kalmar, M. Ferg, Y. Hadzhiev, A. Zaucker, C. Song, S. Schindler, U. Liebel and F. Muller, Automated high-throughput mapping of promoter-enhancer interactions in zebrafish embryos, *Nat. Methods*, 2009, **6**, 911–916.

85 C. Pardo-Martin, T. Y. Chang, B. K. Koo, C. L. Gilleland, S. C. Wasserman and M. F. Yanik, High-throughput in vivo vertebrate screening, *Nat. Methods*, 2010, **7**, 634–636.

86 E. Teixidó, T. R. Kiessling, E. Krupp, C. Quevedo, A. Muriana and S. Scholz, Automated Morphological Feature Assessment for Zebrafish Embryo Developmental Toxicity Screens, *Toxicol. Sci.*, 2019, **167**, 438–449.

87 P. Gut, B. Baeza-Raja, O. Andersson, L. Hasenkamp, J. Hsiao, D. Hesselson, K. Akassoglou, E. Verdin, M. D. Hirschey and D. Y. Stainier, Whole-organism screening for gluconeogenesis identifies activators of fasting metabolism, *Nat. Chem. Biol.*, 2013, **9**, 97–104.

88 B. D. Weger, M. Weger, M. Nusser, G. Brenner-Weiss and T. Dickmeis, A chemical screening system for glucocorticoid stress hormone signaling in an intact vertebrate, *ACS Chem. Biol.*, 2012, **7**, 1178–1183.

89 D. Le, F. Wagner, M. Takamiya, I. L. Hsiao, G. G. Alvaradejo, U. Strähle, C. Weiss and G. Delaittre, Straightforward access to biocompatible poly(2-oxazoline)-coated nanomaterials by polymerization-induced self-assembly, *Chem. Commun.*, 2019, **55**, 3741–3744.

90 Y. Hayashi, M. Takamiya, P. B. Jensen, I. Ojea-Jimenez, H. Claude, C. Antony, K. Kjaer-Sorensen, C. Grabher, T. Boesen, D. Gilliland, C. Oxvig, U. Strähle and C. Weiss, Differential nanoparticle sequestration by macrophages and scavenger endothelial cells visualized in vivo in real-time and at ultrastructural resolution, *ACS Nano*, 2020, **14**, 1665–1681.

91 K. J. Lee, L. M. Browning, P. D. Nallathamby, C. J. Osgood and X. H. Xu, Silver nanoparticles induce developmental stage-specific embryonic phenotypes in zebrafish, *Nanoscale*, 2013, **5**, 11625–11636.

92 P. L. McNeil, D. Boyle, T. B. Henry, R. D. Handy and K. A. Sloman, Effects of metal nanoparticles on the lateral line system and behaviour in early life stages of zebrafish (Danio rerio), *Aquat. Toxicol.*, 2014, **152**, 318–323.

93 D. Xiong, T. Fang, L. Yu, X. Sima and W. Zhu, Effects of nano-scale TiO2, ZnO and their bulk counterparts on zebrafish: acute toxicity, oxidative stress and oxidative damage, *Sci. Total Environ.*, 2011, **409**, 1444–1452.

94 S. P. Yang, O. Bar-Ilan, R. E. Peterson, W. Heideman, R. J. Hamers and J. A. Pedersen, Influence of humic acid on titanium dioxide nanoparticle toxicity to developing zebrafish, *Environ. Sci. Technol.*, 2013, **47**, 4718–4725.

95 T. Xia, M. Kovochich, M. Liong, L. Mädler, B. Gilbert, H. Shi, J. I. Yeh, J. I. Zink and A. E. Nel, Comparison of the mechanism of toxicity of zinc oxide and cerium oxide nanoparticles based on dissolution and oxidative stress properties, *ACS Nano*, 2008, **2**, 2121–2134.

96 B. Bhushan, S. Nandhagopal, K. R. Rajesh and P. Gopinath, Biomimetic nanomaterials: Development of protein coated nanoceria as a potential antioxidative nano-agent for the effective scavenging of reactive oxygen species in vitro and in zebrafish model, *Colloids Surf., B*, 2016, **146**, 375–386.

97 N. Sizochenko, D. Leszczynska and J. Leszczynski, Modeling of Interactions between the Zebrafish Hatching Enzyme ZHE1 and A Series of Metal Oxide Nanoparticles: Nano-QSAR and Causal Analysis of Inactivation Mechanisms, *Nanomaterials*, 2017, **7**, 330.

98 K. J. Ong, X. Zhao, M. E. Thistle, T. J. Maccormack, R. J. Clark, G. Ma, Y. Martinez-Rubi, B. Simard, J. S. Loo, J. G. Veinot and G. G. Goss, Mechanistic insights into the effect of nanoparticles on zebrafish hatch, *Nanotoxicology*, 2014, **8**, 295–304.

99 N. Villamizar, L. M. Vera, N. S. Foulkes and F. J. Sánchez-Vázquez, Effect of lighting conditions on zebrafish growth and development, *Zebrafish*, 2014, **11**, 173–181.

100 A. M. Schoots, R. C. Meijer and J. M. Denucé, Dopaminergic regulation of hatching in fish embryos, *Dev. Biol.*, 1983, **100**, 59–63.

101 Z. Duan, X. Duan, S. Zhao, X. Wang, J. Wang, Y. Liu, Y. Peng, Z. Gong and L. Wang, Barrier function of zebrafish embryonic chorions against microplastics and nanoplastics and its impact on embryo development, *J. Hazard. Mater.*, 2020, **395**, 122621.

102 R. Lehner, C. Weder, A. Petri-Fink and B. Rothen-Rutishauser, Emergence of Nanoplastic in the Environment and Possible Impact on Human Health, *Environ. Sci. Technol.*, 2019, **53**, 1748–1765.

103 C. Della Torre, E. Bergami, A. Salvati, C. Faleri, P. Cirino, K. A. Dawson and I. Corsi, Accumulation and embryotoxicity of polystyrene nanoparticles at early stage of development of sea urchin embryos Paracentrotus lividus, *Environ. Sci. Technol.*, 2014, **48**, 12302–12311.

104 A. Pinsino, E. Bergami, C. Della Torre, M. L. Vannuccini, P. Addis, M. Secci, K. A. Dawson, V. Matranga and I. Corsi, Amino-modified polystyrene nanoparticles affect signalling pathways of the sea urchin (Paracentrotus lividus) embryos, *Nanotoxicology*, 2017, **11**, 201–209.

105 L. F. Marques-Santos, G. Grassi, E. Bergami, C. Faleri, T. Balbi, A. Salis, G. Damonte, L. Canesi and I. Corsi, Cationic polystyrene nanoparticle and the sea urchin immune system: biocorona formation, cell toxicity, and multixenobiotic resistance phenotype, *Nanotoxicology*, 2018, **12**, 847–867.

106 I. Brandts, M. Teles, A. Tvarijonaviciute, M. L. Pereira, M. A. Martins, L. Tort and M. Oliveira, Effects of polymethylmethacrylate nanoplastics on Dicentrarchus labrax, *Genomics*, 2018, **110**, 435–441.

107 S. Bhargava, S. S. Chen Lee, L. S. Min Ying, M. L. Neo, S. Lay-Ming Teo and S. Valiyaveettil, Fate of Nanoplastics in Marine Larvae: A Case Study Using Barnacles, Amphibalanus amphitrite, *ACS Sustainable Chem. Eng.*, 2018, **6**, 6932–6940.

108 A. M. Booth, B. H. Hansen, M. Frenzel, H. Johnsen and D. Altin, Uptake and toxicity of methylmethacrylate-based nanoplastic particles in aquatic organisms, *Environ. Toxicol. Chem.*, 2016, **35**, 1641–1649.

109 D. M. Mitrano, A. Beltzung, S. Frehland, M. Schmiedgruber, A. Cingolani and F. Schmidt, Synthesis of metal-doped nanoplastics and their utility to investigate fate and behaviour in complex environmental systems, *Nat. Nanotechnol.*, 2019, **14**, 362–368.

110 D. Cassano, R. La Spina, J. Ponti, I. Bianchi and D. Gilliland, Inorganic Species-Doped Polypropylene Nanoparticles for Multifunctional Detection, *ACS Appl. Nano Mater.*, 2021, **4**, 1551–1557.

111 A. Delgado-Gonzalez, E. Garcia-Fernandez, T. Valero, M. V. Cano-Cortes, M. J. Ruedas-Rama, A. Unciti-Broceta, R. M. Sanchez-Martin, J. J. Diaz-Mochon and A. Orte, Metallofluorescent Nanoparticles for Multimodal Applications, *ACS Omega*, 2018, **3**, 144–153.

